Protein delivery into live cells by incubation with an endosomolytic agent

Alfredo Erazo-Oliveras*, Kristina Najjar*, Laila Dayani, Ting-Yi Wang, Gregory A. Johnson and Jean-Philippe Pellois

Figure S1. Structure and expected mass of fTAT.

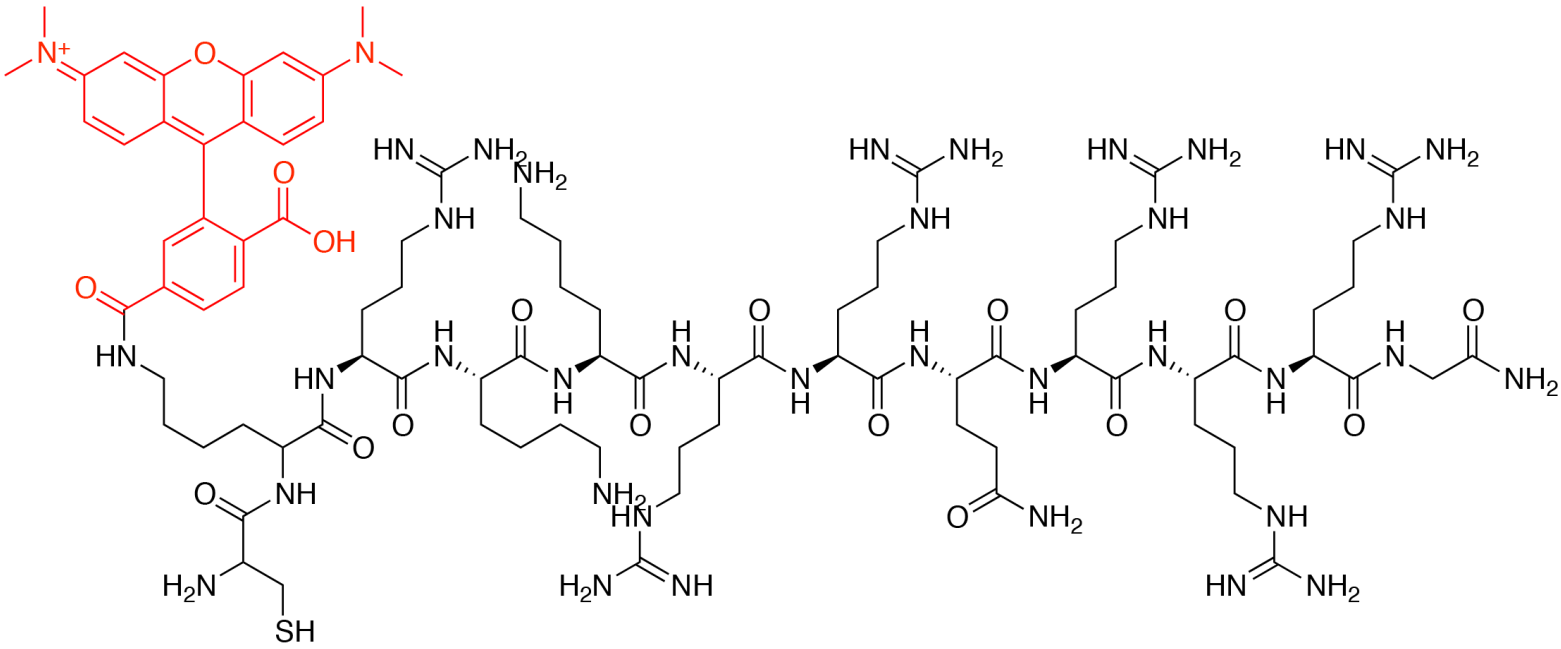

Exact mass: 2040.43

Figure S2. Structure and expected mass of dfTAT.

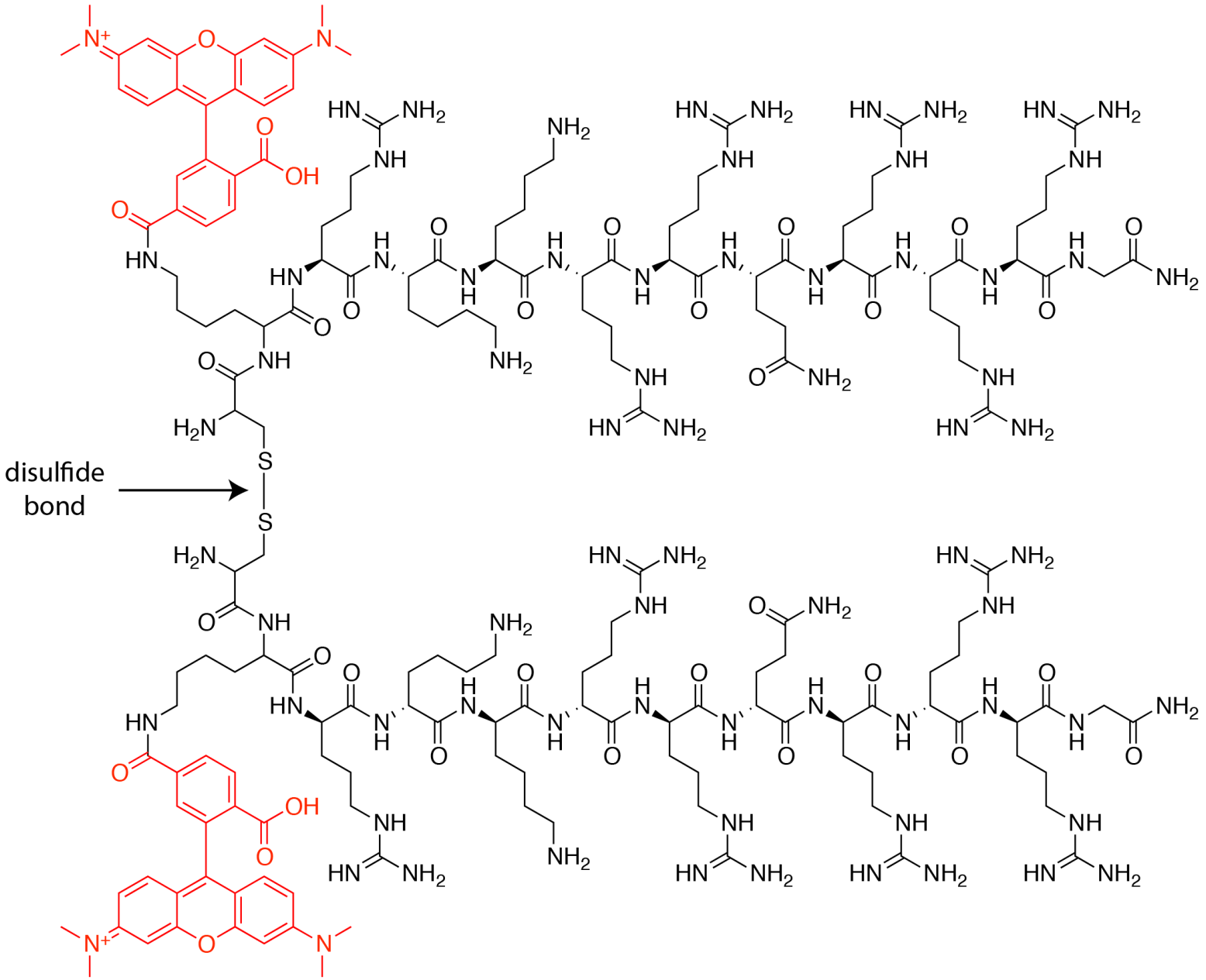

Exact mass: 4080.34

Figure S3. Characterization of fTAT and dfTAT

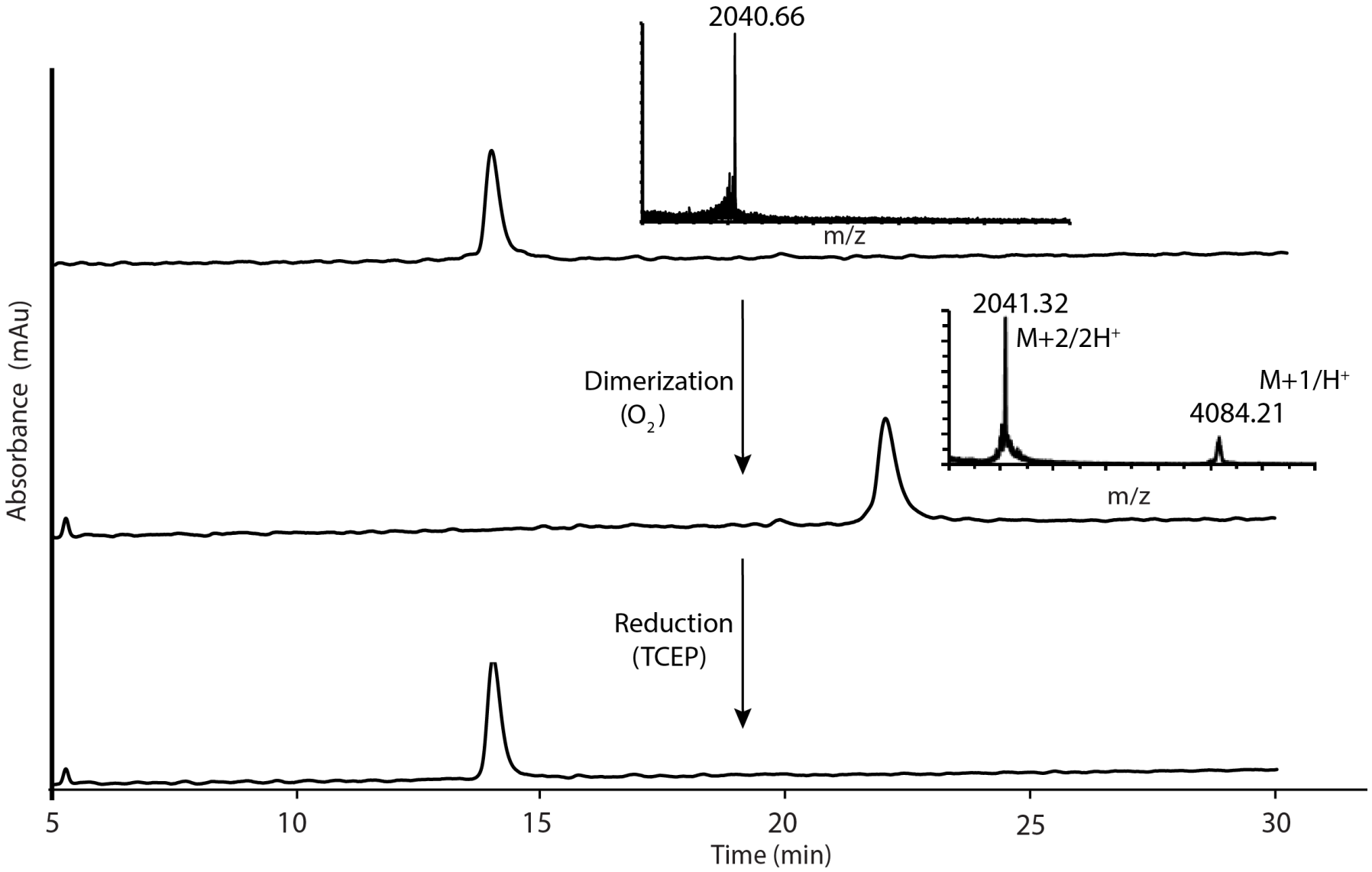

(a) HPLC analysis and MALDI-TOF MS spectrum of purified CK(ε-NH-TMR)TATG (fTAT) (retention time (rt): 14.2 min) (fTAT, expected mass = 2041.17, observed mass = 2040.66) (b) HPLC analysis and MALDI-TOF MS spectrum of purified dfTAT. dfTAT was obtained by incubating fTAT in oxygenated buffer overnight. After HPLC purification, dfTAT shows a single peak with a rt = 22.7 min. (dfTAT, expected mass = 4080.34, observed mass: M+1/1H+ = 4084.21 Da M+2/2H+ = 2041.32) (c) HPLC analysis of reduction reaction of dfTAT after addition of the reducing agent tris(2-carboxyethyl)phosphine (TCEP). Pure dfTAT was mixed with a solution of TCEP (50 mM) in water and allowed to react for 15 min. The HPLC chromatogram show a peak with rt = 14.3 min and is identical to the retention time of pure fTAT.

Figure S4. Structure and expected mass of acfTAT.

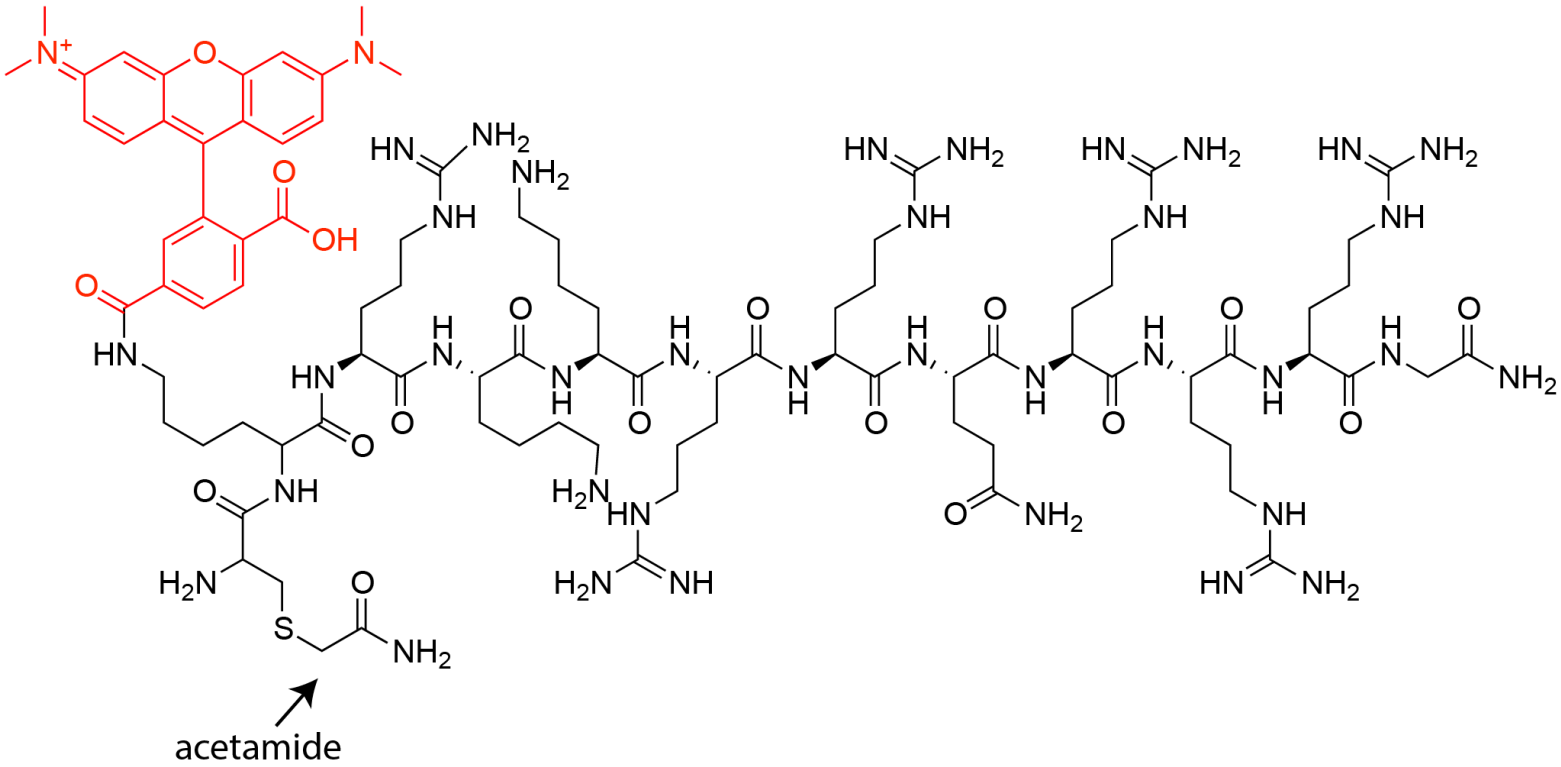

Exact mass: 2098.19

Figure S5. Characterization of acfTAT

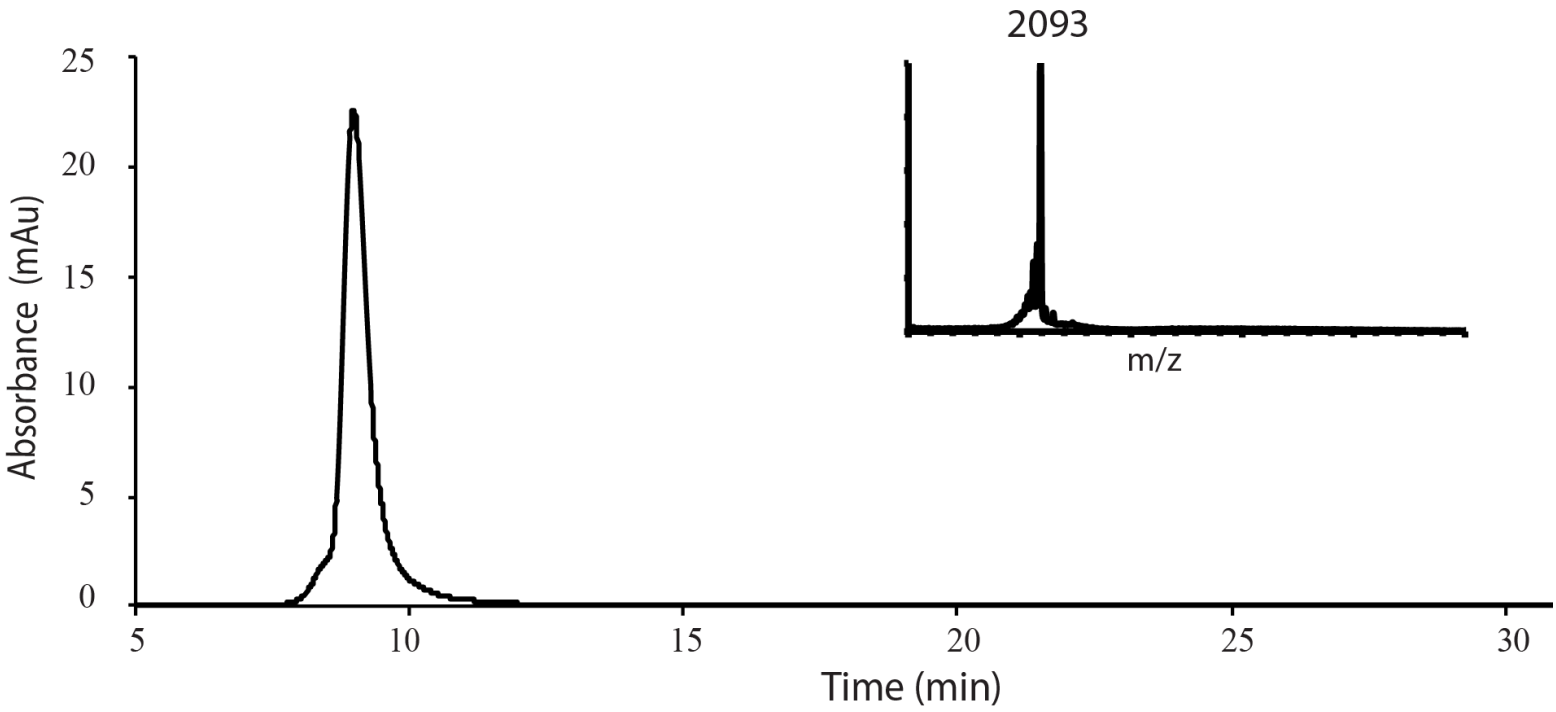

HPLC analysis and MALDI-TOF MS spectrum of pure acfTAT (rt = 8.93 min) (expected mass: 2098.19, observed mass: 2096.31).

Figure S6. Characterization and delivery of nrdfTAT

a)

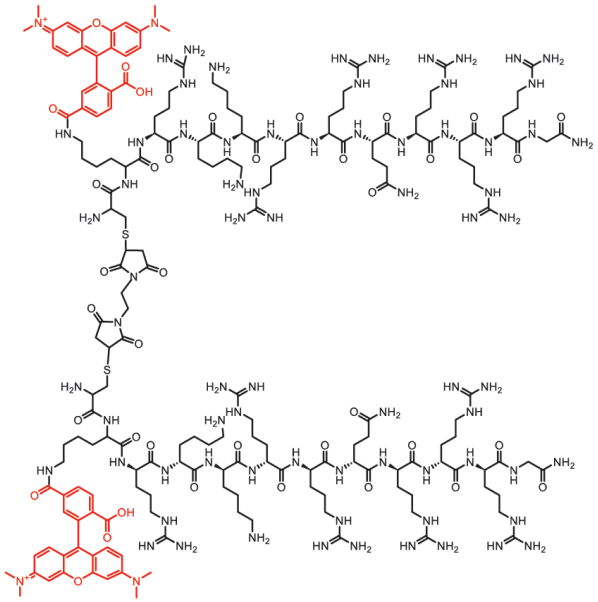

Exact mass: 4313.39

b)

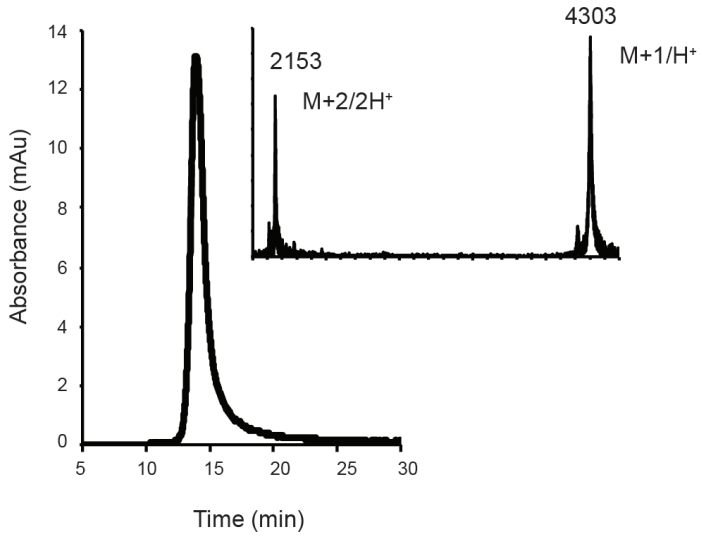

c)

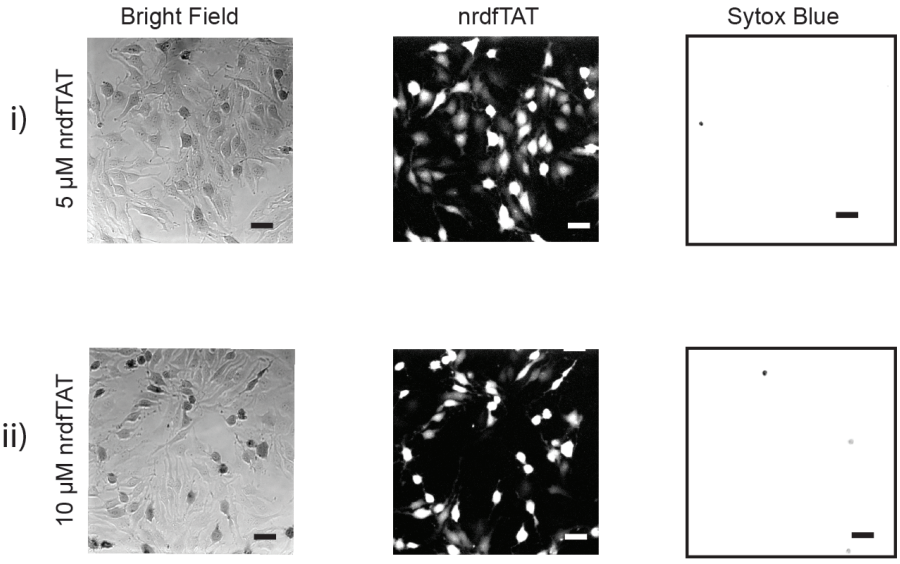

(a) Structure and expected mass of nrdfTAT (b) HPLC analysis and MALDI-TOF mass spectrum of purified nrdfTAT (rt: 13.9min, expected mass = 4313.39, observed mass= 4303) (d) Cytosolic delivery of nrdfTAT into live cells. HeLa cells were incubated with nrdfTAT ((i) 2.5-5 µM and (ii) 5-10 µM *) for 1h. Fluorescence images (monochrome (white=fluorescence signal, black=no signal) 20X image, center panel) show cytosolic delivery of nrdfTAT into HeLa cells at both concentrations. SYTOX Blue (2 µM) was used as an indicator of cell death. Scale bars, 50 µm (Inverted monochrome 20X image).

* The concentration of nrdfTAT was estimated by measuring the absorbance of TMR using a spectrophotometer, as described with other peptides. However, nrdfTAT has two TMR spaced by a 8.0 Å BMOE linker and such close proximity might affect the extinction coefficient of TMR. In order to take this effect into account, a concentration range for nrdfTAT was calculated based on the extinction coefficient of free TMR (91,500 mol-1cm-1) and that of dfTAT (45,500 mol-1cm-1) (dfTAT also has two TMR in close proximity).

Figure S7. Cytosolic and nuclear fluorescence distribution of dfTAT is concentration dependent.

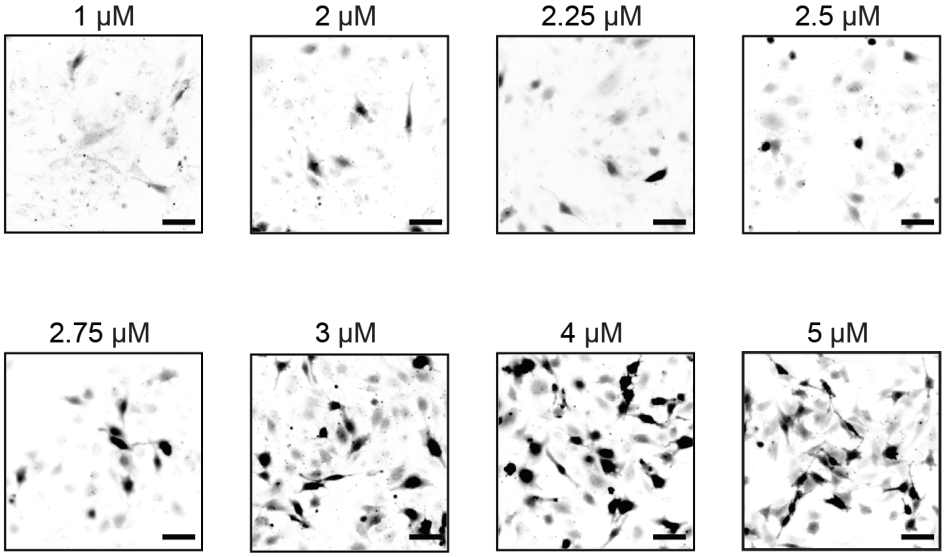

HeLa cells were incubated with varying concentration of dfTAT (1, 2, 2.5, 2.25, 2.5, 2.75, 3, 4, 5 μM). Cells were washed and imaged. Inverted monochrome images (20X objective) show a dramatic increase in the cytosolic delivery of the peptide between 2-5 μM. Although not shown here, the number of cells in each image is approximately the same as determined by bright field imaging. Cells that display a fluorescence punctate distribution are not clearly visible under these imaging conditions. Further analysis of these cells using a 100X objective clearly show a fluorescence punctate distribution indicative of peptide trapped in endosomes. Scale bars, 50 μm.

Figure S8. Delivery of dfTAT into the cytosol and nucleus of live cells was achieved in multiple cell lines.

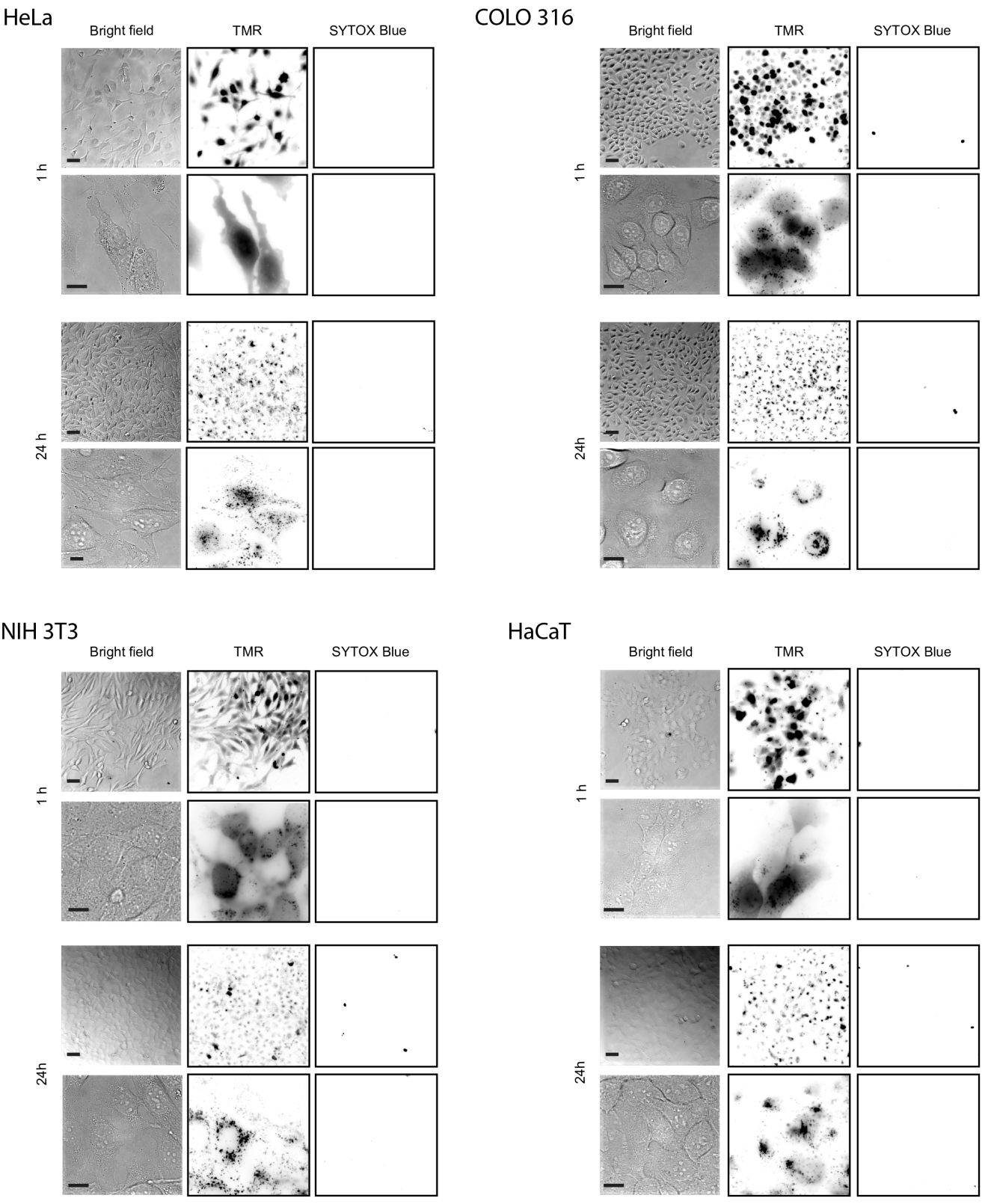

The cell lines HeLa, NIH 3T3, COLO 316 and HaCaT were incubated with 5 µM dfTAT for 1 h, washed and imaged. The fluorescence signal detected was in the cytosol and nucleus of cells (top panel: 20X objective, bottom panel: 100X objective). After imaging, cells were incubated at 37 °C in a humidified atmosphere containing 5% CO2 for 24 h, washed and imaged again (top panel: 20X objective, bottom panel: 100X objective). The cell morphology did not change after 24 h. Cell viability is assessed by exclusion of the cell-impermeable nuclear stain SYTOX Blue at both 1h and 24 h time point. The TMR fluorescence at the 24 h time point is different to that obtained at the 1 h time point presumably because of the intracellular degradation of the peptide. Scale bars, 20X objective: 50 µm; 100X objective: 10 µm.

Figure S9. Delivery of dfTAT into the cytosol and nucleus of live cells was achieved in multiple cell lines.

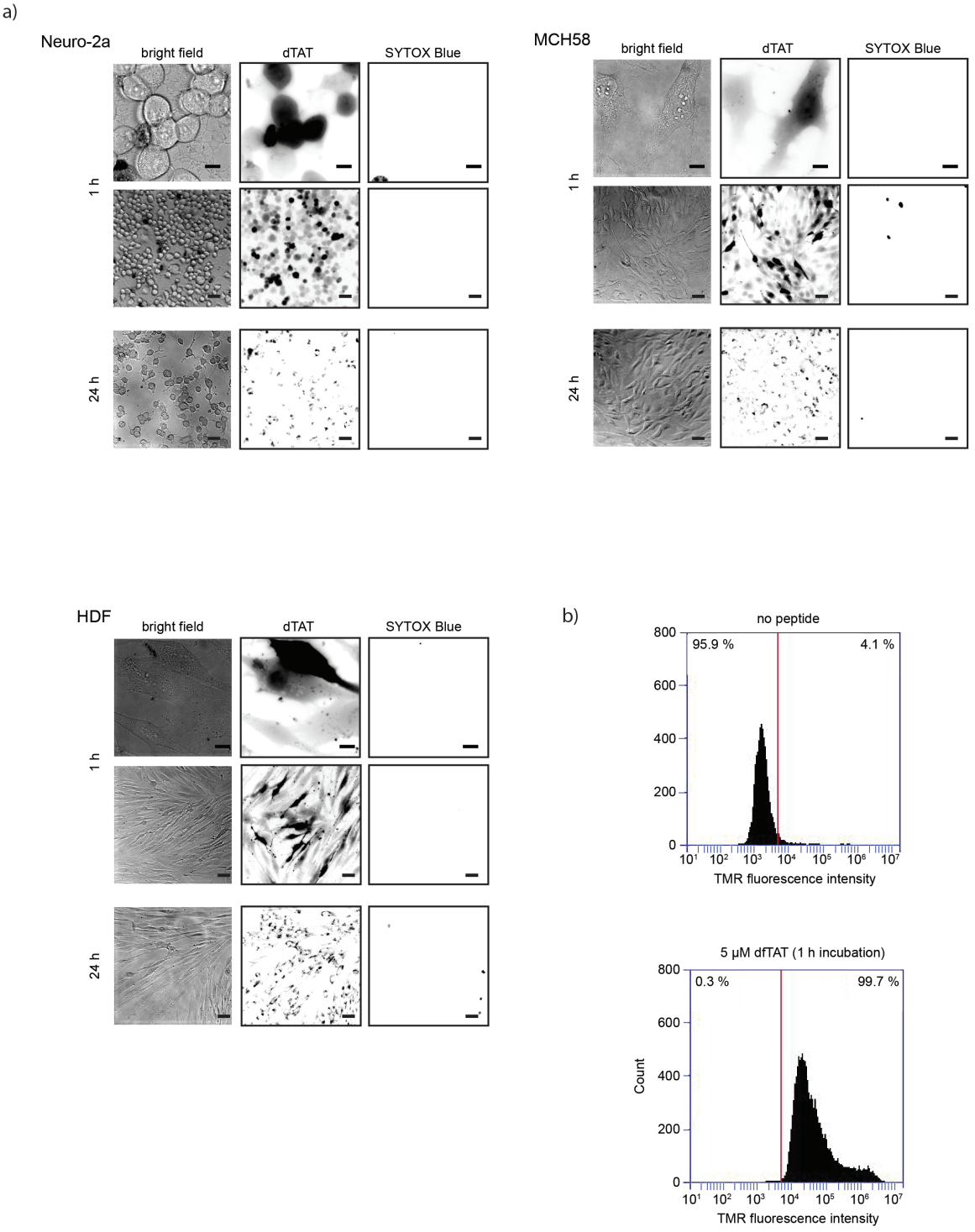

(a) The cell lines Neuro-2a, HDF and MCH58 were incubated with 5 µM dfTAT for 1 h, washed and imaged. The fluorescence signal detected was in the cytosol and nucleus of cells (top panel: 100X objective, bottom panel: 20X objective). After imaging, cells were incubated at 37 °C in a humidified atmosphere containing 5% CO2 for 24 h, washed and imaged (20X objective). Bright field images show that the morphology of cells 24 h after incubation is identical to that of cells imaged immediately after incubation. Cell viability is assessed by exclusion of the cell-impermeable nuclear stain SYTOX Blue at both 1h and 24 h time point. The TMR fluorescence at the 24 h time point is different to that obtained at the 1 h time point presumably because of the intracellular degradation of the TAT peptide and release of the TMR fluorophore. Scale bars, 20X objective: 50 µm; 100X objective: 10 µm. (b) Histogram of flow cytometry data. HeLa cells were incubated with 5 µM dfTAT or no peptide (control) for 1h. Cells were then trypsinized for 5 min, resuspended in a total of 200 µl of nrL-15, and analyzed by flow cytometry (BD Accuri C6 Flow Cytometer). Histograms show that 99.7 % of cells contained red fluorescence.

Figure S10. Delivery of dfTAT into the cytosol and nucleus of primary intestinal porcine epithelial cells (IPEC-1).

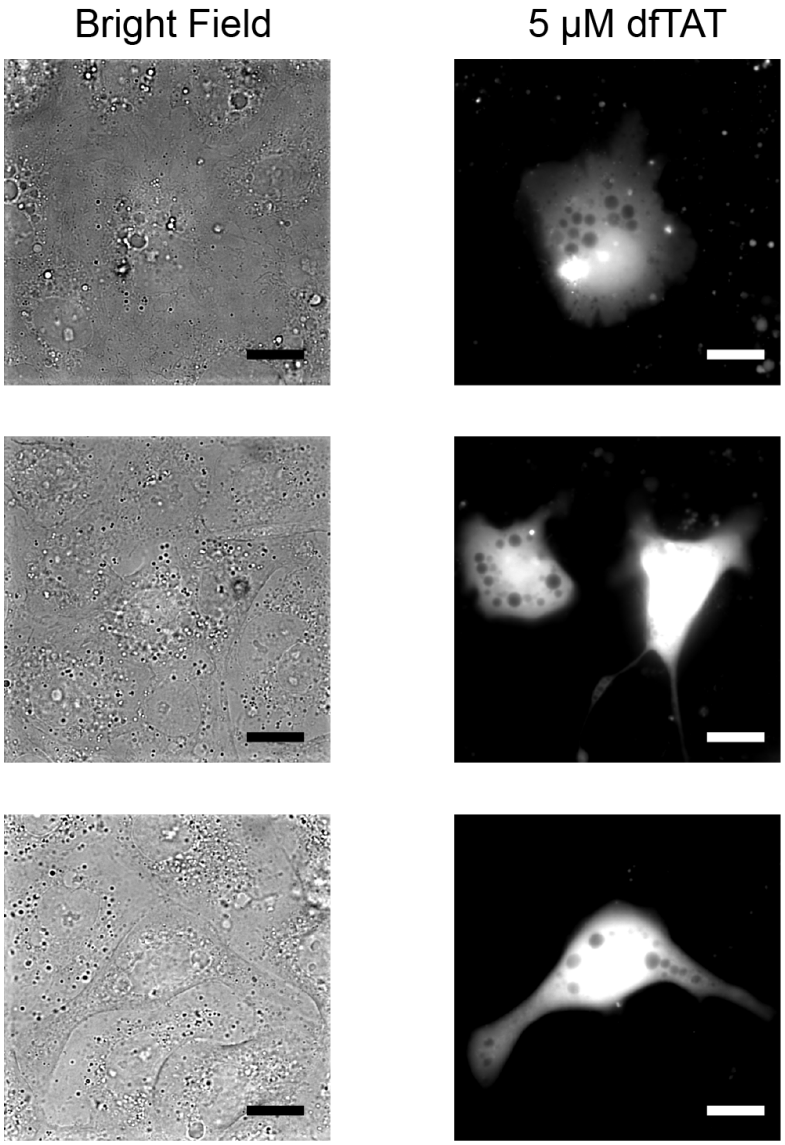

Cells were incubated with 5 µM dfTAT for 1h, washed and then imaged. Fluorescence (monochrome) images show cytosolic and nuclear distribution of dfTAT in IPEC-1 cells. Scale bars: 10 µm.

Figure S11. fTAT cellular localization after incubation with live cells depends on its concentration in the extracellular media.

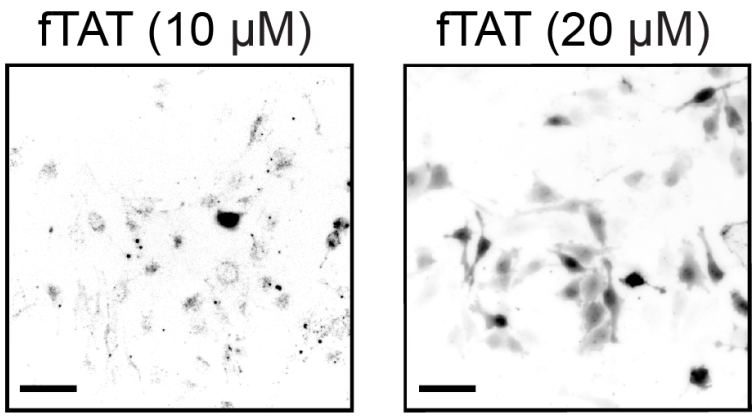

Inverted monochrome (black=fluorescence signal, white=no signal) fluorescence images of HeLa cells incubated with 10 or 20 μM of fTAT for 1 h. fTAT displays at fluorescence punctate distribution at 10 μM fTAT (left panel) while at 20 μM fTAT shows a significant increase in the population of cells displaying cytosolic and nuclear fluorescence distribution. Scale bars, 50 μm.

Figure S12. Fluorescence emission spectra of dfTAT (5 μM) before and after reduction with the reducing agent TCEP (50 mM).

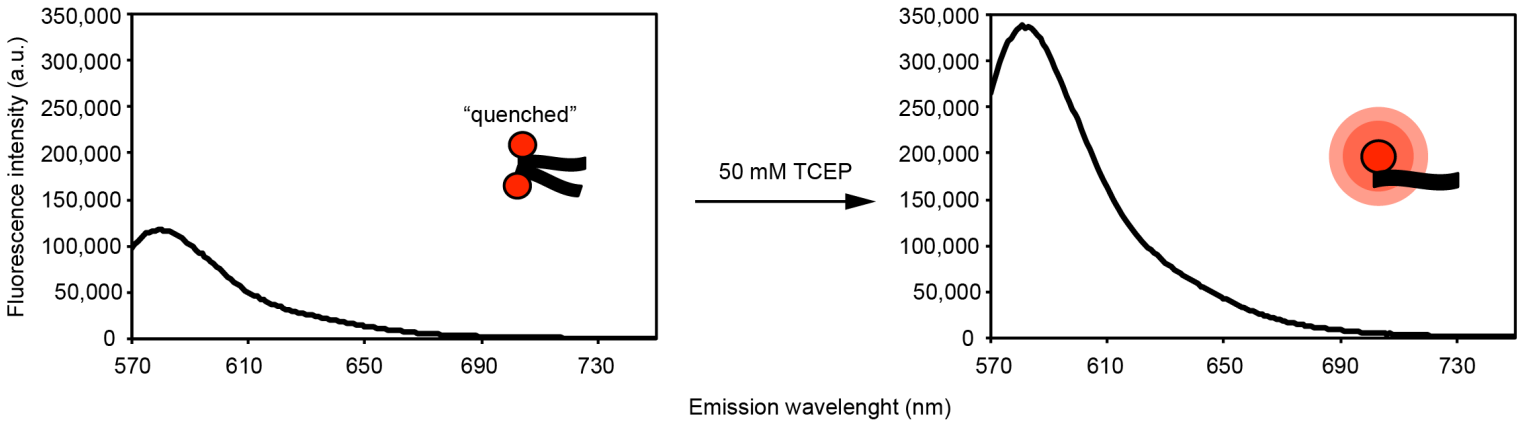

The sample was excited at 556 nm and the emission was recorded between 570-750nm. The emission spectra show that the fluorescence emission of dfTAT increases upon reduction of its disulfide bond. This is indicative of TMR self-quenching in the context of dfTAT.

Figure S13. Structure and characterization of DEAC-K9.

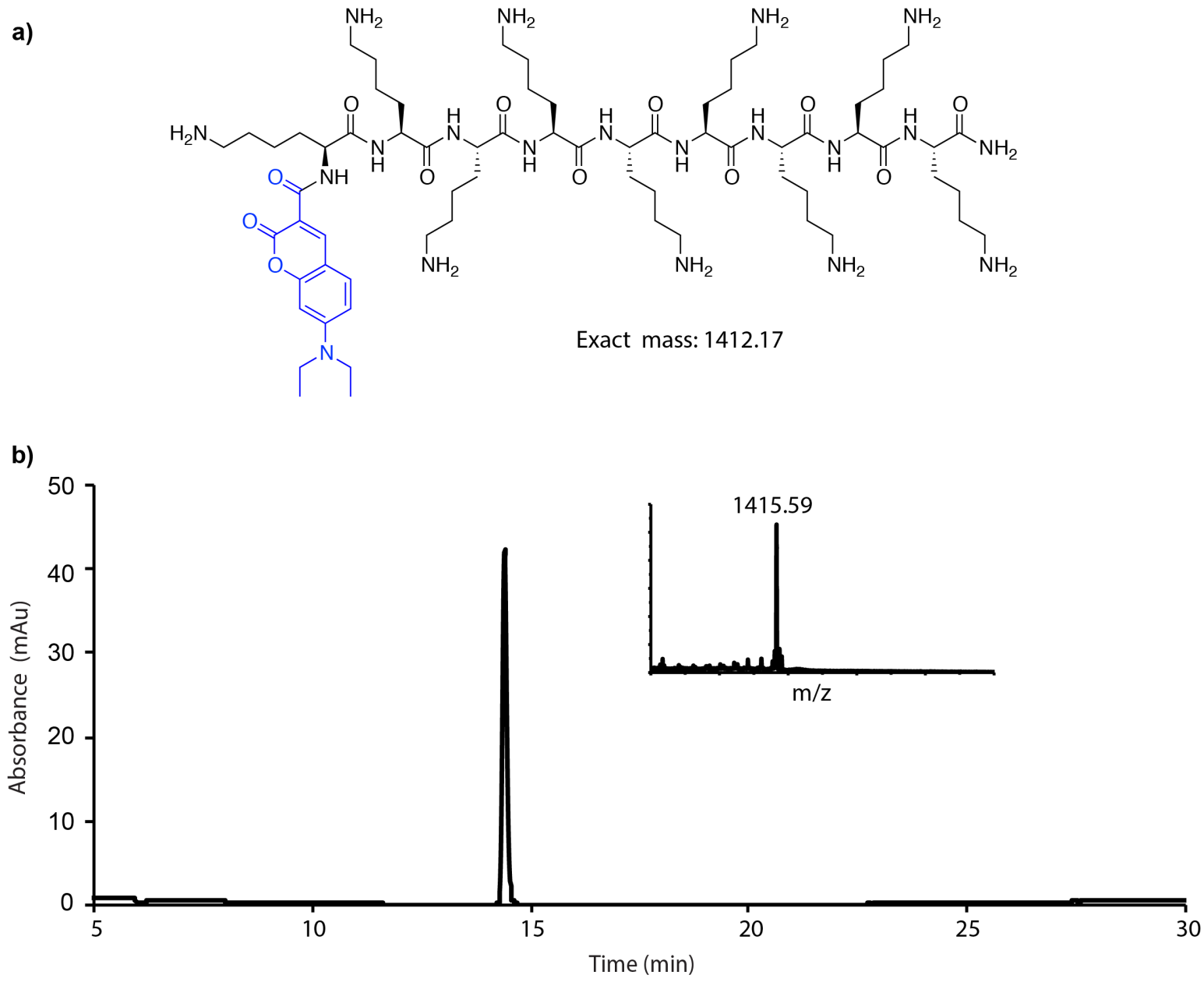

(a) Structure and expected mass of DEAC-K9. (b) Characterization of DEAC-K9. HPLC analysis and MALDI-TOF MS spectrum of pure DEAC-K9 (rt = 14.40 min) (expected mass: 1412.97, observed mass: 1415.59)

Figure S14. dfTAT displays a high endosomolytic activity when compared to acfTAT.

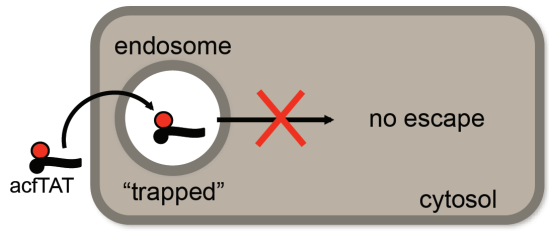

Why does dfTAT penetrate the cytosol of cells when acfTAT and fTAT do not?

Model 1

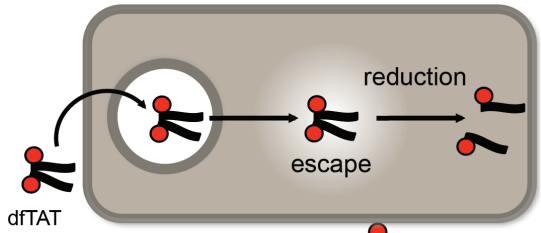

dfTAT penetration is possible if is more endosomolytic than

Model 2

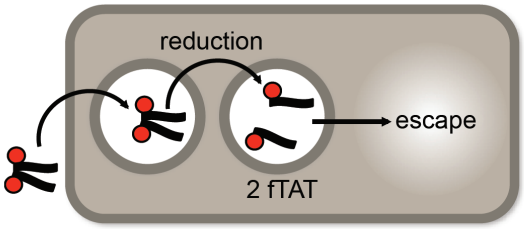

dfTAT penetration is possible if [ ] < [ ]
inside endosomes: reduced dfTAT and acfTAT are equally endosomolytic but the endocytic uptake of dfTAT is such that more peptide accumulates inside endosomes, thereby reaching a "penetration" threshold.

Design:

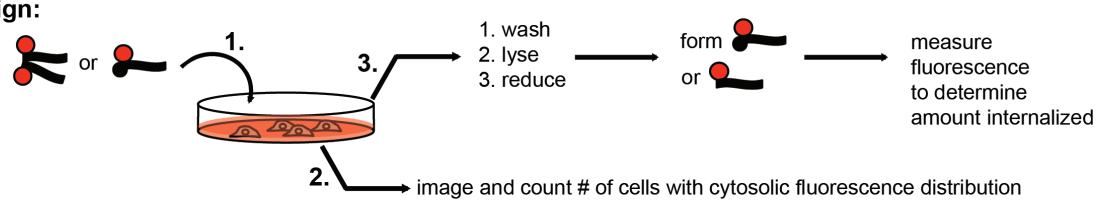

Results:

	peptide in media (μM)	fluorescence intensity of cell lysate (a.u.)	estimated average peptide concentration per cell (mM)	cells with cytosolic fluorescence distribution (%)
dfTAT	5	986.8	0.65 if or 1.3 if	76.9
acfTAT	50	1208.4	1.6	5.6

numbers used for calculations: number of cells in sample (measured by flow cytometry) = 80,000
estimated volume of a cell = 2 10^{-12} L (bionumbers.hms.harvard.edu)
calibration with samples of known concentration: fluorescence intensity = 326.5 x [TAT in μM]

Conclusions:

When dfTAT is internalized by cells at a lower level then acfTAT (this requires a large concentration of acfTAT in media in comparison to dfTAT), dfTAT penetrates the cytosol of cells but acTAT remains trapped inside endosomes. This is inconsistent with model 2 and instead supports model 1.
Additional information supporting model 1:
1) the number of endosomes present in cells treated with dfTAT (2 μM, below escape threshold) , fTAT, or acfTAT is approximately equal (100-400) based on fluorescence microscopy (this supports the notion that the total amount of peptide internalized by cells can be correlated to the concentration inside endosomes comparably between experiments).
2) nrdfTAT, a dimer that cannot be reduced inside endosomes, has an activity similar to dfTAT.
3) endosomes can be non-reducing (this is cell-type dependent) and disulfide bonds have been demonstrated to be stable inside endocytic organelles of HeLa cells (Lee YJ *et al* J Am Chem Soc. 2008 Feb 27;130(8):2398-9).

HeLa cells were incubated with dfTAT (5 μM) for 5 min and acfTAT (50 μM) for 1 h. After 1 h, the cells were washed with PBS/heparin, imaged and lysed. The lysis buffer used in this experiment contains 2 mM DTT. The bulk fluorescence of cell lysates on a 96-well plate was measured using a plate reader. The fluorescence of each sample was normalized to total protein content in the cell lysate, as determined by a Bradford protein assay. Similarly, the fluorescence of solutions of acfTAT at different concentrations (0.1, 0.5, 1, 5 and 10 μM) was measured using a plate reader. A calibration curve of the peptide fluorescence intensity v.s. peptide concentration was established. These data was used to estimate the average concentration of acfTAT and dfTAT inside cells. Data shows higher fluorescence intensity for acfTAT than dfTAT inside cells. These data suggests that dfTAT is a dimer inside endosomes and that this peptide is more endosomolytic than acfTAT (Model 1).

Figure S15. Peptide overall uptake in HeLa cells as a function of the concentration of peptide present in the media.

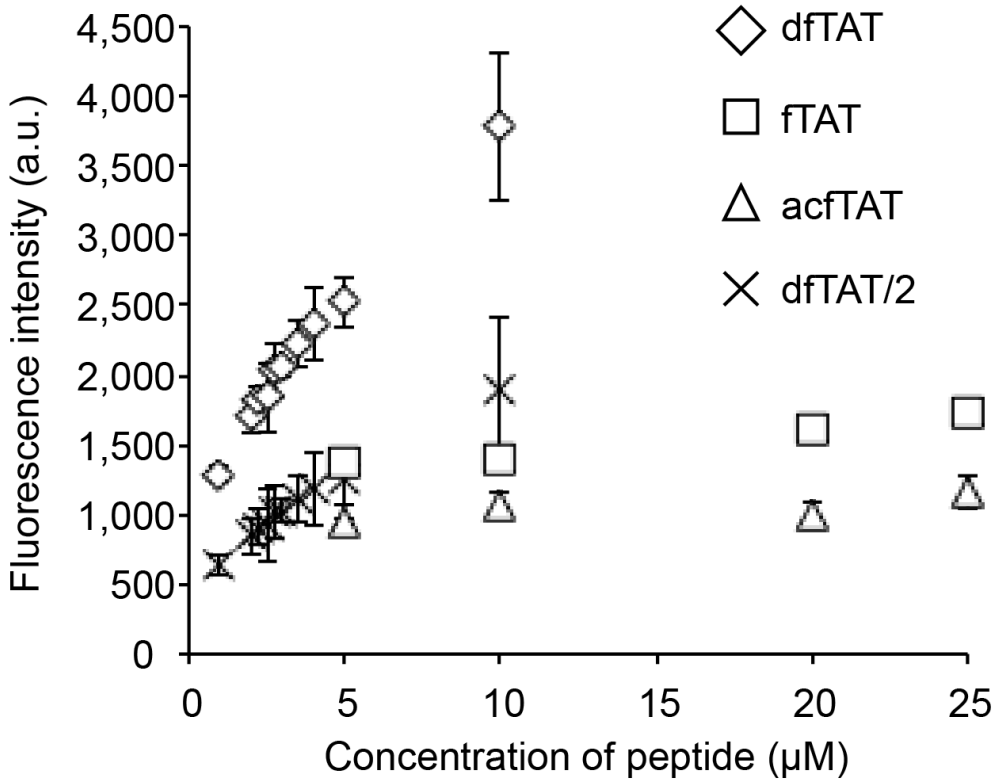

The uptake of the three peptides by HeLa cells was measured as a function of concentration (μM). Cells were incubated with either acfTAT (5-25 μM), fTAT (5-25 μM) or dfTAT (1-10 μM) and the bulk fluorescence of cell lysates on a 96-well plate was measured using a plate reader. The fluorescence of each sample was normalized to total protein content in the cell lysate, as determined by a Bradford protein assay. Data shows a linear increase in the fluorescence uptakeof cells incubated with dfTAT. The lysis buffer used in this experiment contains 2 mM DTT. dfTAT is reduced to the monomeric fTAT upon this treatment. Consequently, the normalized fluorescence of dfTAT was divided by two (dfTAT/2) to compare the uptake of dfTAT to that of fTAT (the signal of one molecule of dfTAT gives a signal twice that of a molecule of internalized fTAT in this assay).

Figure S16. SNAP-Surface 488 enters cells via endocytosis.

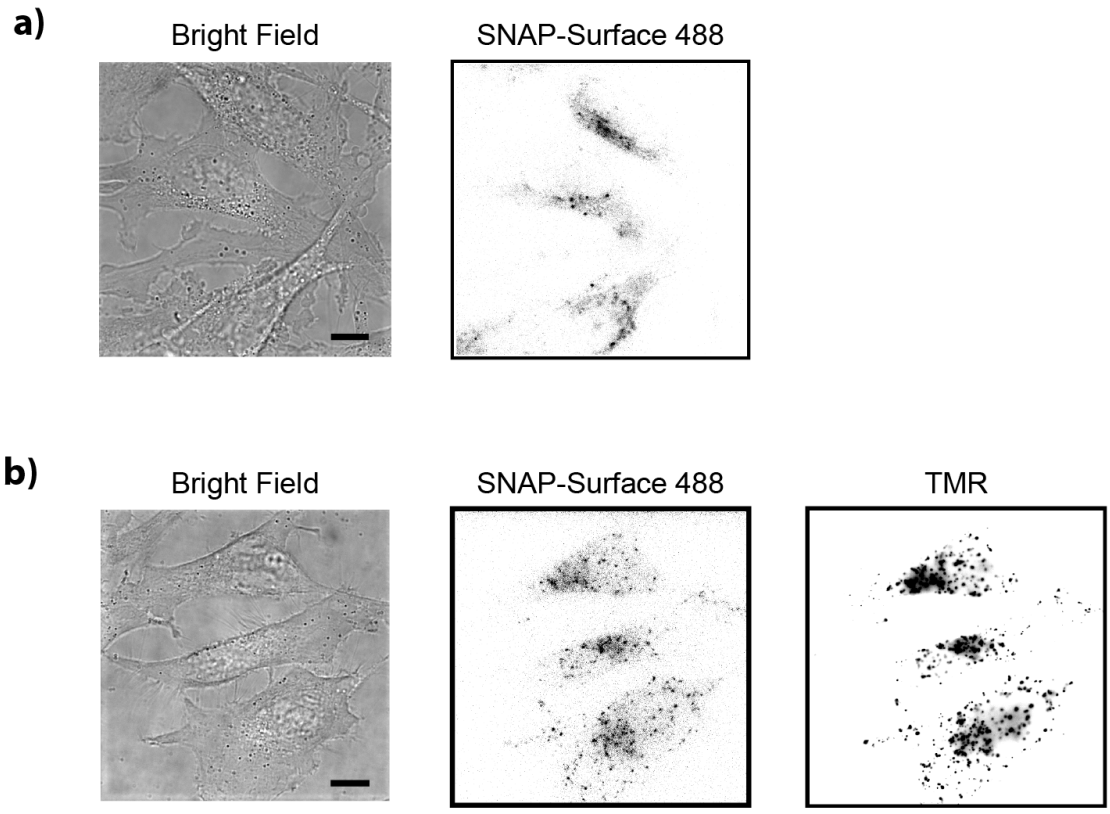

(a) HeLa cells were incubated with 5 µM SNAP-Surface 488 for 1 h, washed and imaged. Inverted monochrome image shows a punctate fluorescence distribution from SNAP-Surface 488 (right panel). (b) HeLa cells were incubated with 5 µM SNAP-Surface 488 and 2.5 µM dfTAT (a concentration in which dfTAT incubation does not result in significant cytosolic release) for 1h, washed and imaged. Inverted monochrome image shows SNAP-Surface 488 accumulation in endocytic organelles (punctate distribution) (right panel) and colocalization with TMR signal. Bright field images show HeLa cells morphology did not change after uptake of SNAP-Surface 488 and/or dfTAT (right panels). Scale bars, 10 µm.

Figure S17. dfTAT is not toxic to cells under conditions where efficient endosomal escape is achieved.

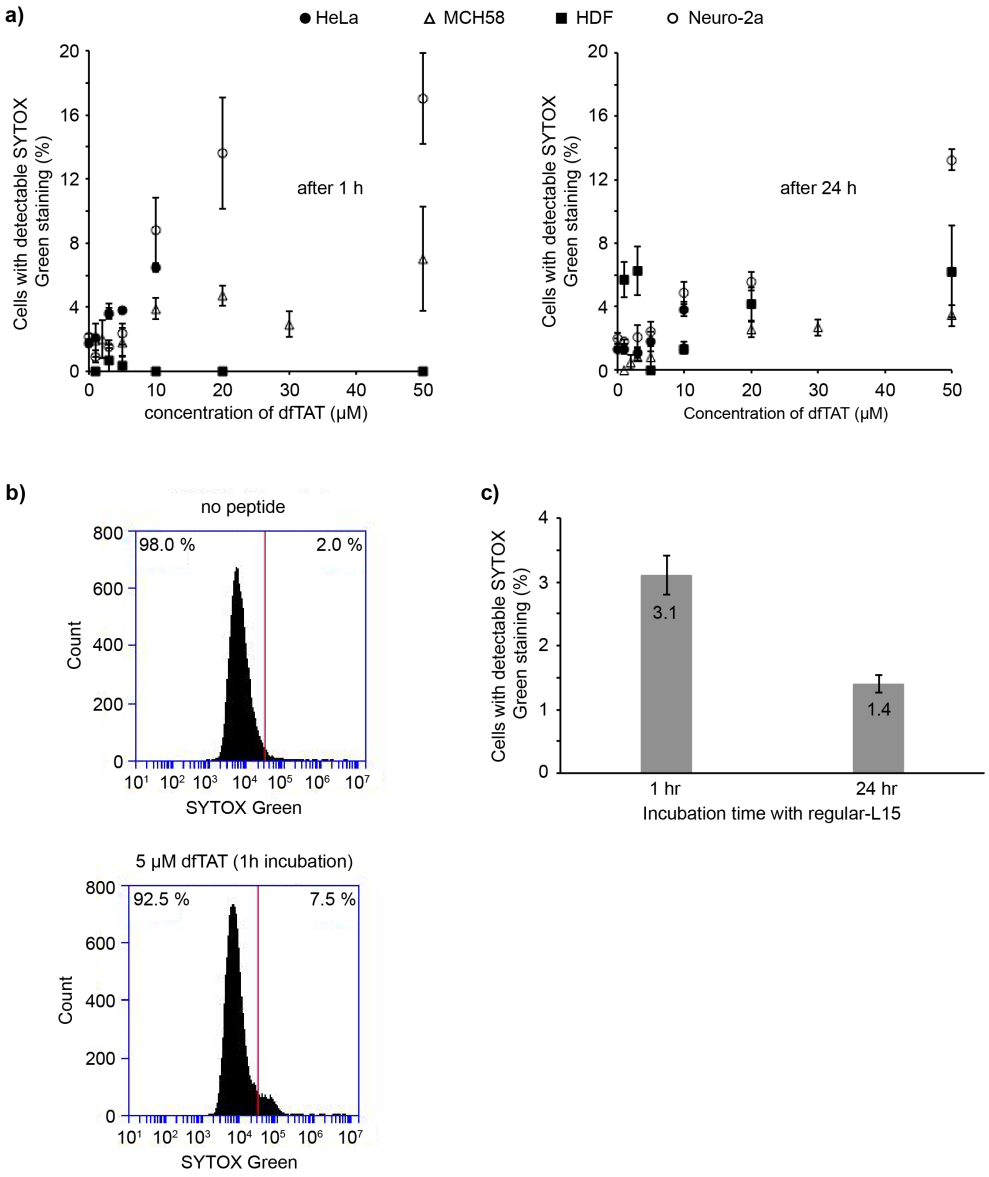

(a) HeLa, MCH58, HDF and Neuro-2a cells were incubated with (1-50 μM) dfTAT for 1 h. Cell viability was assessed by a SYTOX Green exclusion assay 1, 24, and 48 h (for HeLa) after incubation (1,000 cells/experiment, experiments in triplicates, average and standard deviations represented). (b) Histogram of flow cytometry data. HeLa cells were incubated with 5 μM dfTAT or no peptide (control) for 1h, washed and then incubated in SYTOX Green (1 μM) for 15 min. Cells were then trypsinized for 5 min, resuspended in a total of 200 μl of nrL-15, and analyzed by flow cytometry (BD Accuri C6 Flow Cytometer). Histograms show that only 2% and 7.5% of cells are stained with the cell impermeable dye SYTOX Green for untreated and treated cells, respectively. (c) HeLa cells were incubated with 5 μM dfTAT for 1h in the presence of regular-L15, washed and then incubated in SYTOX Green (2 μM) for 15 min. Cells were imaged using fluorescence microscopy to determined the amount of cells stained with SYTOX Green. Bar graph shows that 1 hr and 24 hr after incubation only 3.1 % and 1.4 % of the cell population was stained with the dye, respectively.

Figure S18. The cellular localization of acfTAT and dfTAT is different after incubation with live cells.

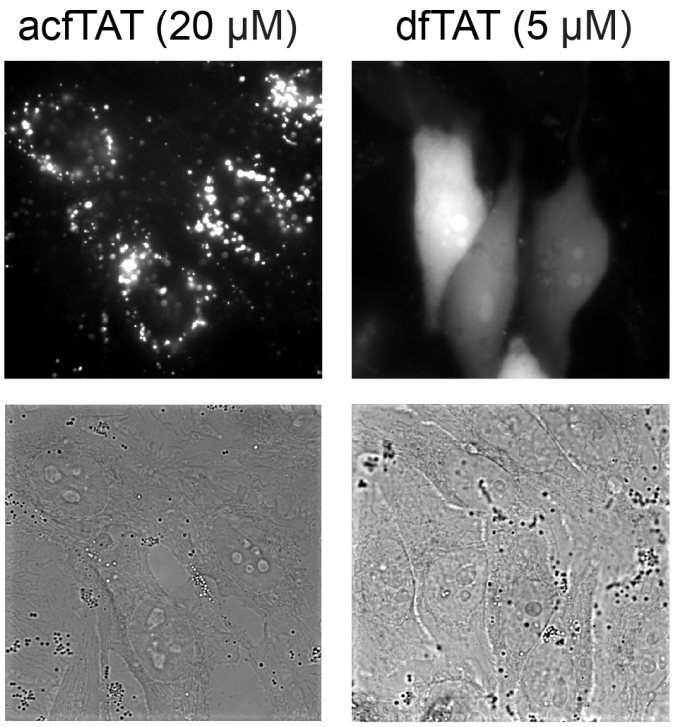

(a) Fluorescence (monochrome) and bright field images (100X objective) of HeLa cells incubated with 20 μM acfTAT (left panel) and 5 μM dfTAT (right panel). The acfTAT peptide displays a fluorescence punctate distribution while dfTAT exhibits a cytosolic and nuclear fluorescence distribution. Bright field images show no change in HeLa cell morphology upon peptide delivery. Scale bar, 10 μm.

Figure S19. mRNA expression analysis in the presence of staurosporine.

a) Staurosporine 1h incubation

Gene names related to apoptosis	FC	Log2 FC
Homo sapiens baculoviral IAP repeat-containing 5 (BIRC5), transcript variant 1, mRNA.	8.67	3.12
Homo sapiens cell division cycle 2, G1 to S and G2 to M (CDC2), transcript variant 1, mRNA.	5.64	2.5
Homo sapiens topoisomerase (DNA) II alpha 170kDa (TOP2A), mRNA.	4.98	2.31
Homo sapiens breast cancer 1, early onset (BRCA1), transcript variant BRCA1-delta11b, mRNA.	2.99	1.58
Homo sapiens breast cancer 1, early onset (BRCA1), transcript variant BRCA1-delta14-17, mRNA.	2.94	1.55
Homo sapiens cell division cycle 2, G1 to S and G2 to M (CDC2), transcript variant 1, mRNA.	2.89	1.53
Homo sapiens potassium large conductance calcium-activated channel, subfamily M, alpha member 1 (KCNMA1), transcript variant 2, mRNA.	2.76	1.46
Homo sapiens baculoviral IAP repeat-containing 5 (BIRC5), transcript variant 3, mRNA.	2.53	1.34

21 transcripts out of a total 47321 transcripts

Gene names related to apoptosis	FC	Log2 FC
Homo sapiens tumor necrosis factor (ligand) superfamily, member 14 (TNFSF14), transcript variant 2, mRNA.	0.48	-1.06
Homo sapiens hypoxia-inducible factor 1, alpha subunit (basic helix-loop-helix transcription factor) (HIF1A), transcript variant 2, mRNA.	0.47	-1.09
Homo sapiens hypoxia-inducible factor 1, alpha subunit (basic helix-loop-helix transcription factor) (HIF1A), transcript variant 1, mRNA.	0.47	-1.09
Homo sapiens BCL2/adenovirus E1B 19kDa interacting protein 3-like (BNIP3L), mRNA.	0.45	-1.15
Homo sapiens suppressor of cytokine signaling 2 (SOCS2), mRNA.	0.41	-1.29
Homo sapiens msh homeobox 1 (MSX1), mRNA.	0.36	-1.47
Homo sapiens DNA-damage-inducible transcript 3 (DDIT3), mRNA.	0.35	-1.51
Homo sapiens v-myc myelocytomatosis viral oncogene homolog (avian) (MYC), mRNA.	0.32	-1.64
Homo sapiens interleukin 10 (IL10), mRNA.	0.32	-1.64
Homo sapiens v-myc myelocytomatosis viral oncogene homolog (avian) (MYC), mRNA.	0.29	-1.79
Homo sapiens immediate early response 3 (IER3), mRNA.	0.28	-1.84
Homo sapiens cyclin-dependent kinase inhibitor 1A (p21, Cip1) (CDKN1A), transcript variant 2, mRNA.	0.25	-2
Homo sapiens heat shock 70kDa protein 5 (glucose-regulated protein, 78kDa) (HSPA5), mRNA.	0.24	-2.06

b)

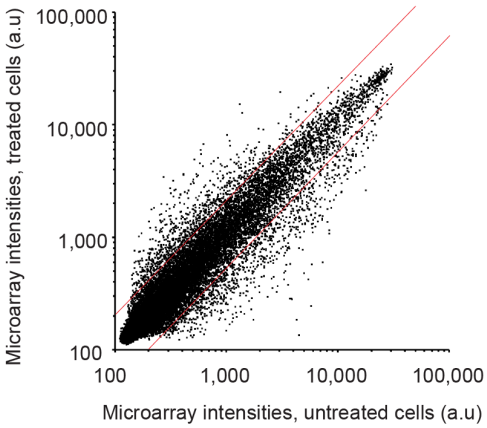

c)

dfTAT 5 μM, 1h incubation

Gene name	Fold change(FC)	Log2 FC
PREDICTED: Homo sapiens misc_RNA (LOC148430), miscRNA.	2.04	1.03
Homo sapiens ornithine decarboxylase antizyme 2 (OAZ2), mRNA.	2.04	1.03
Homo sapiens immediate early response 3 (IER3), mRNA.	0.49	-1.03
Homo sapiens glutaminase (GLS), mRNA.	0.49	-1.03
Homo sapiens cDNA FLJ31351 fis, clone MESAN2000167	0.48	-1.06
Homo sapiens early growth response 1 (EGR1), mRNA.	0.46	-1.12
Homo sapiens growth differentiation factor 15 (GDF15), mRNA.	0.43	1.21
PREDICTED: Homo sapiens similar to mCG49427 (LOC100129882), mRNA.	0.42	-1.25
Homo sapiens microRNA 221 (MIR221), microRNA.	0.39	1.36
Homo sapiens early growth response 2 (Krox-20 homolog, Drosophila) (EGR2), mRNA.	0.35	-1.51
Homo sapiens dual specificity phosphatase 6 (DUSP6), transcript variant 2, mRNA.	0.32	-1.64

11 transcripts out of a total 47321 transcripts

dfTAT 5 μM, 1h + 1h after incubation

Gene name	FC	Log2 FC
Homo sapiens FBJ murine osteosarcoma viral oncogene homolog B (FOSB), mRNA.	2.4	1.26
PREDICTED: Homo sapiens misc_RNA (LOC148430), miscRNA.	0.46	-1.12

2 transcripts out of a total 47321 transcripts

dfTAT 5 μM, 1h+ 24 h after incubation

Gene name	FC	Log2 FC
PREDICTED: Homo sapiens similar to aggrecan 1 isoform 2 precursor (LOC649366), mRNA.	0.5	-1
Homo sapiens dehydrogenase/reductase (SDR family) member 3 (DHRS3), mRNA.	0.36	-1.47

2 transcripts out of a total 47321 transcripts

(a) In order to establish a positive control for the microarray analysis, staurosporin was used to induce apoptosis in HDF cells. Cells were treated with staurosporine (0.1 μM) for 1h and mRNA levels were analyzed as described in Figure 3. The identity of transcripts related to apoptosis that were up-regulated (highlighted in red) and down-regulated (highlighted in green) upon treatment with staurosporin are listed. Notably, a total of 1830 transcripts were found to be up-or down-regulated out of 47321 transcripts detected. (b) Analysis of the microarray intensities of untreated HDF cells vs. those of HDF cells treated with staurosporine (0.1 μM) for 1h. The red lines represent the 2-fold cut-offs. (c) Table listing the identity of transcripts that are up-regulated (highlighted in red) and down-regulated (highlighted in green) in HDF cells incubated with dfTAT (5 μM) and analyzed immediately after incubation (1h), or 1h (1h+1h) and 24 h (1h+24h) after incubation. The 11, 2, and 2 transcripts listed represent the total number of transcripts up or down-regulated in the 1h, 1h+1h, and 1h+24h samples, respectively.

Figure S20. DIGE proteomic analysis of HDF cells treated with dfTAT (5 μM) for 1 h.

a)

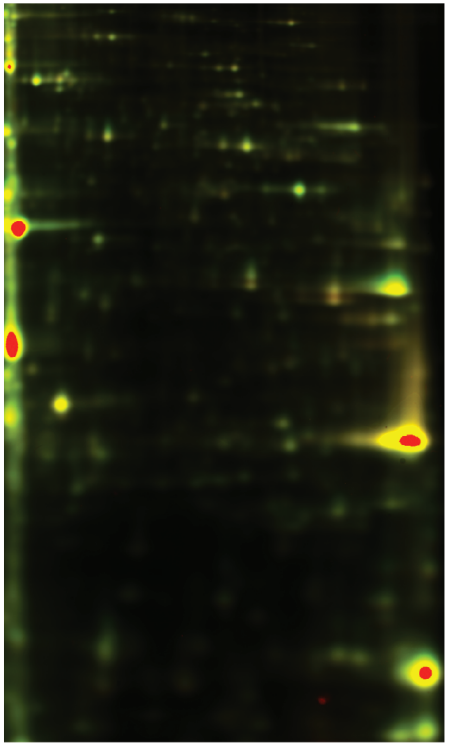

b)

	1+0h	1+1h	1+24h
	# spots (%)	# spots (%)	# spots (%)
Decreased	29 (6.8%)	12 (2.3%)	23 (4.2%)
Similar	391 (91.8%)	487 (94.9%)	488 (90%)
Increased	6 (1.4%)	14 (2.7%)	31 (5.7%)
Total number of spots included	426	513	542

(a) Representative green and red fluorescence overlay of 2D gel of cells treated with or without dfTAT for 1h and incubated in fresh media for an additional 1h (1+1h samples, treated sample is labeled with Cy3 and untreated with Cy5). Green and red were used as pseudo colors for Cy3 and Cy5 dyes, respectively, and a yellow color is indicative of equal fluorescence intensities. (b) Table summarizing analysis results obtained from the DIGE using the DeCyder v6.5 suite of software tools (GE Healthcare). Data was obtained using a 2 standard deviation model (95% confidence). Each pair (treated vs. untreated) were individually analyzed based on the normalized volume ratio of each individual protein spot from Cy3- or Cy5- labeled sample.

Figure S21. dfTAT mediates delivery of two cargos simultaneously inside live cells.

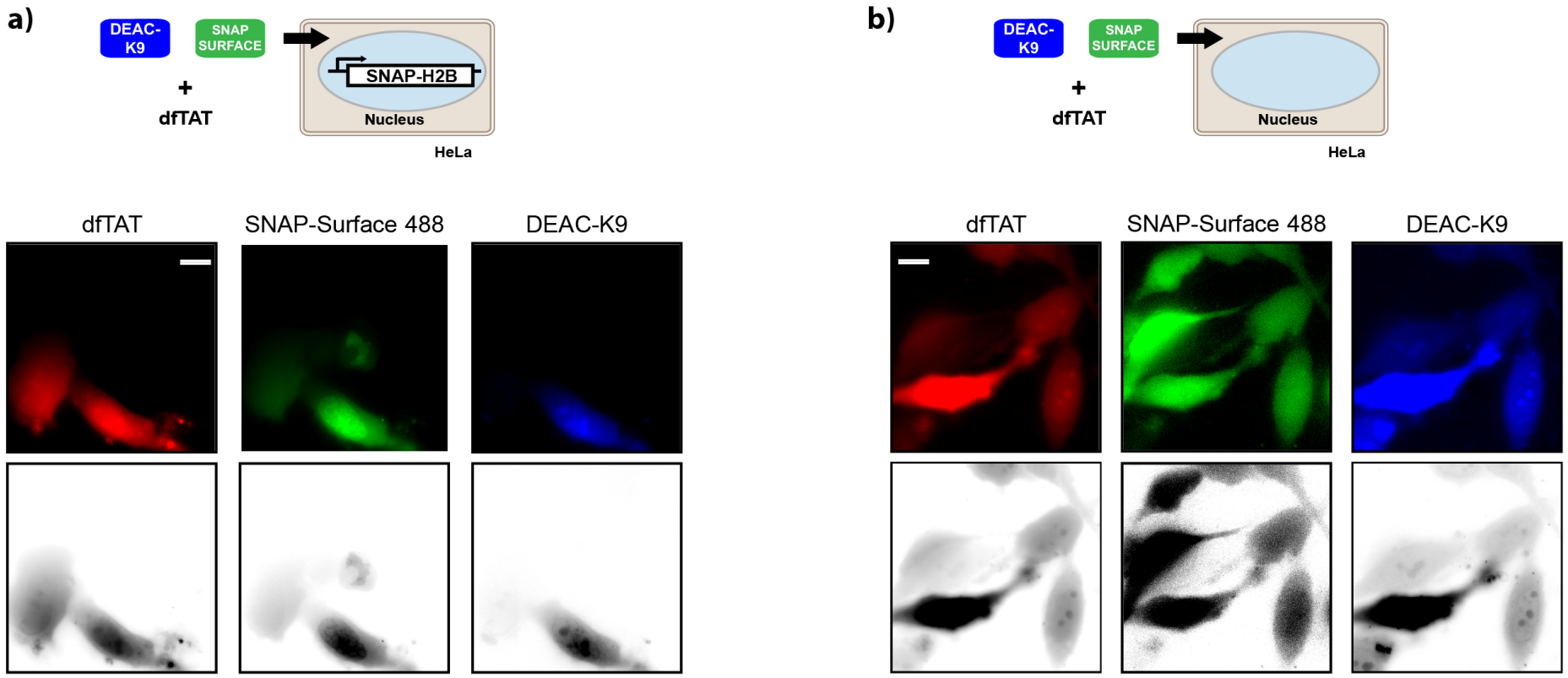

(a) HeLa cells expressing SNAP-H2B were incubated with 5 μM dfTAT, 5 μM SNAP-Surface 488 and 5 μM DEAC-K9. Fluorescence images (RGB and inverted monochrome) show cytosolic and nuclear localization of dfTAT (red fluorescence), DEAC-K9 (blue fluorescence) and SNAP-Surface 488 (green fluorescence). Moreover, the SNAP-Surface signal accumulated in the nucleus as shown in Figure 2c. (b) HeLa cells were incubated with 5 μM dfTAT, 5 μM SNAP-Surface 488 and 5 μM DEAC-K9. Fluorescence and inverted monochrome images show cytosolic and nuclear fluorescence localization of dfTAT (red fluorescence), DEAC-K9 (blue fluorescence) and SNAP- Surface 488 (green fluorescence). Scale bars, 10μm.

Figure S22. Delivery of SNAP-Surface 488 did not occur in the absence of dfTAT during the two-step delivery protocol.

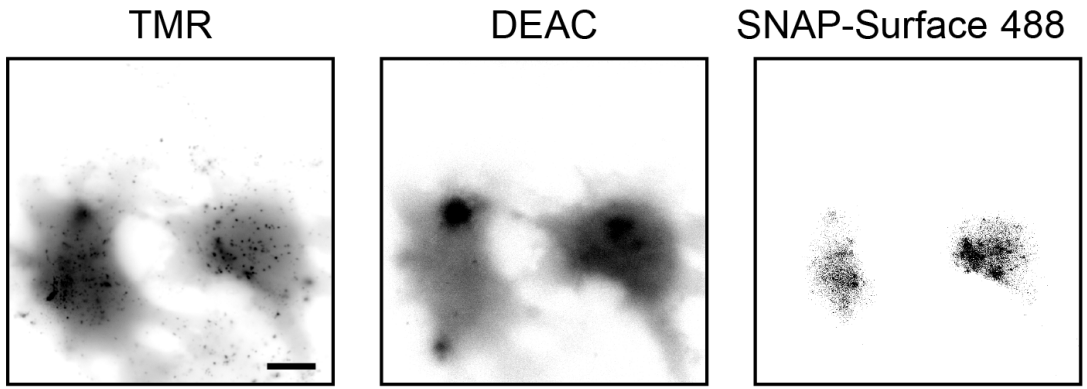

HeLa cells were first incubated with 5 μM dfTAT and 5 μM DEAC-K9 for 1 h. Cells were then washed, incubated with 5 μM SNAP-Surface 488 for 1 h and imaged. In one hand, inverted monochrome images show cytosolic and nuclear localization of TMR and DEAC but, in the other hand, SNAP-Surface 488 display a fluorescence punctate distribution. Scale bar, 10μm.

Figure S23. dfTAT mediated delivery of intact EGFP into different cell lines.

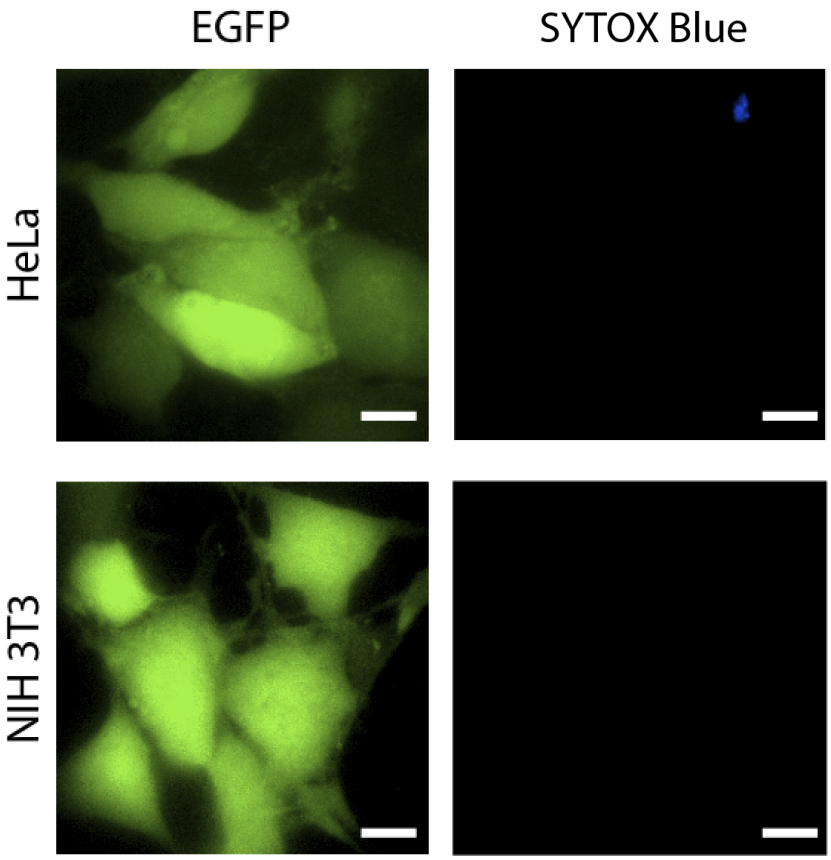

HeLa (top panel) and NIH 3T3 (bottom panel) cells were incubated with EGFP (10 μM) and dfTAT(5 μM) for 1 h, washed and imaged. Images show a homogenous cytosolic fluorescence distribution of EGFP in HeLa and NIH 3T3 cells. Scale bars, 10 μm.

Figure S24. dfTAT mediated delivery of intact EGFP into HeLa and primary HDF cells.

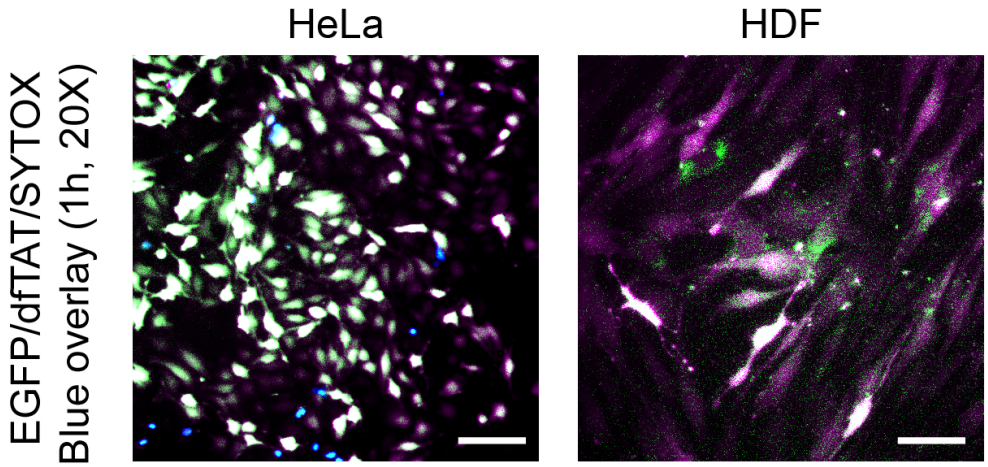

HeLa and primary HDF cells were incubated with EGFP (10 μM) and dfTAT (5 μM) for 1 h, washed and imaged. Images show a homogenous cytosolic fluorescence distribution of EGFP and dfTAT in HeLa and primary HDF cells. Scale bars, 50 μm.

Figure S25. Quantitation of the concentration of EGFP delivered into the cytosol of HDF and Neuro-2a.

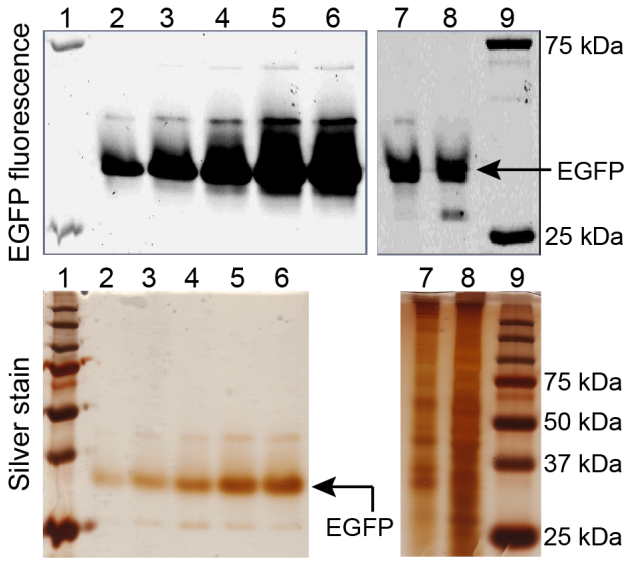

lane	sample
1	protein ladder
2	100 nM EGFP
3	200 nM EGFP
4	400 nM EGFP
5	800 nM EGFP
6	1000 nM EGFP
7	HDF cell lysate
8	Neuro-2a cell lysate
9	protein ladder

	EGFP in media (μM)	fluorescence intensity of EGFP band in gel from the cell lysate (a.u.)	amount of EGFP in the cell lysate (nM)	estimated average of EGFP concentration per cell (μM)
HDF	10	12100	110.2	34.6
Neuro-2a	10	3900	49.6	23.3

numbers used for calculation: number of cells in sample (measured by flow cytometry) = 79,600
estimated volume of a cell = 2 10^{-12} L (bionumbers.hms.harvard.edu)

HDF and Neuro-2a cells were co-incubated with dfTAT (5 μM) and EGFP (10 μM) for 1 h. After 1 h, cells were wash with PBS/heparin and lysed. The cell lysate was treated with nucleases and an aliquot of 27 μL was analyzed by PAGE (top right panel). Similarly, samples of known EGFP concentrations (determined by measuring absorbance at 488 nm and using an extinction coefficient of 55,000 mol-1cm-1) were analyzed by PAGE (top left panel). A fluorescence imager was used to measure the EGFP fluorescence intensity from the cell lysates and EGFP calibration samples. Silver staining was used to detect all proteins in the lysate. A calibration curve of EGFP fluorescence intensity vs. EGFP concentration was established and used to estimate the average concentration of EGFP in the cell lysates. The data obtained was used to calculate the concentration of EGFP per cell. Important numbers: Cell number on well: 79,600 (determined by flow cytometry); Cell volume: 2000 μm3 (bionumbers.hms.harvard.edu.)

Figure S26. The amount of DEAC-K9 delivered into cells can be titrated.

a)

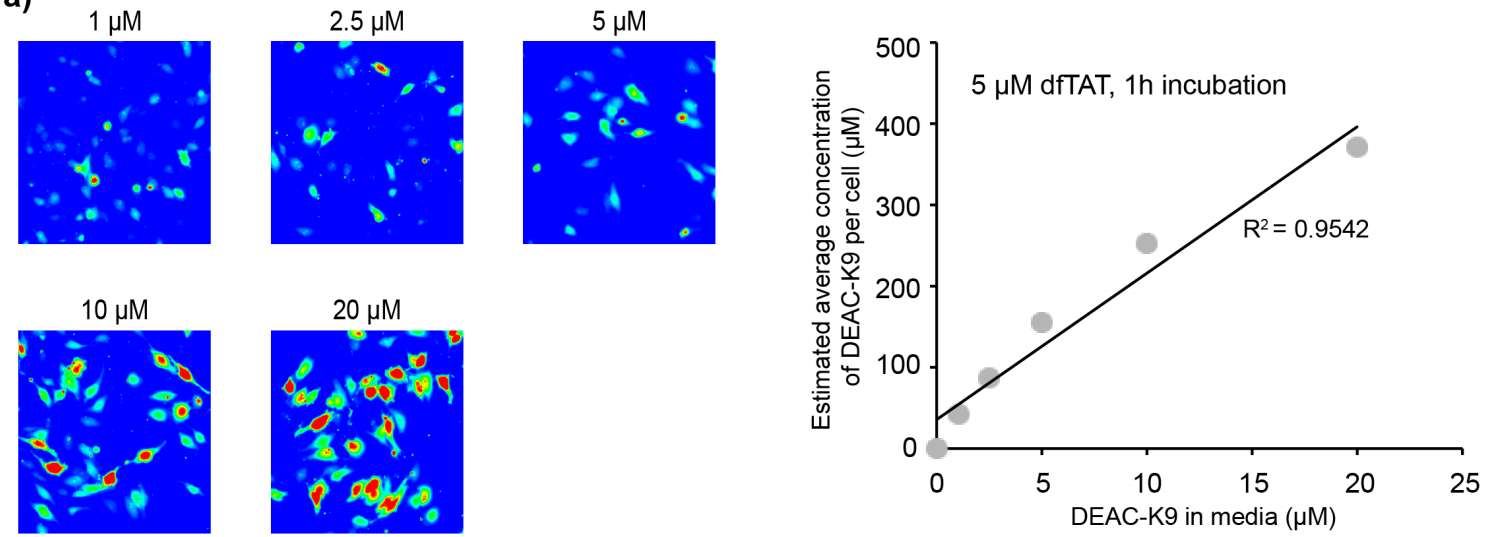

b)

peptide in media (μM)	fluorescence intensity of cell lysate (a.u.)	DEAC-K9 concentration in the cell lysate (nM)	estimated average concentration of DEAC-K9 per cell (μM)
1	2793.4	67.1	42.1
2.5	5745.9	138.0	86.6
5	10352.8	248.6	156.0
10	16817.2	403.9	253.4
20	24544.1	589.5	369.9

HeLa cells were incubated with dfTAT (5 μM) and different concentrations of DEAC-K9 (1, 2.5, 5, 10 and 20 μM) for 1 h. Cells were wash with PBS/heparin, imaged and lysed. The bulk fluorescence of cell lysates containing DEAC-K9 was measured using a fluorometer. Similarly, the fluorescence of solutions of DEAC-K9 at different concentrations (0.01. 0.1, 1, 10 and 100 μM) was measured using a fluorometer. A calibration curve of DEAC-K9 intensity vs. DEAC-K9 concentration was established. These data was used to estimate the average concentration of DEAC-K9 inside cells. Data shows a linear increase in the amount of DEAC-K9 delivered inside cells (top right panel). Consistent with these data, fluorescence images that show an increase in the fluorescence signal in the cytosol cells with increasing concentrations o DEAC-K9 incubated in the media (top left panel, and Figure 5).

Figure S27. dfTAT and EGFP do not interact when co-incubated.

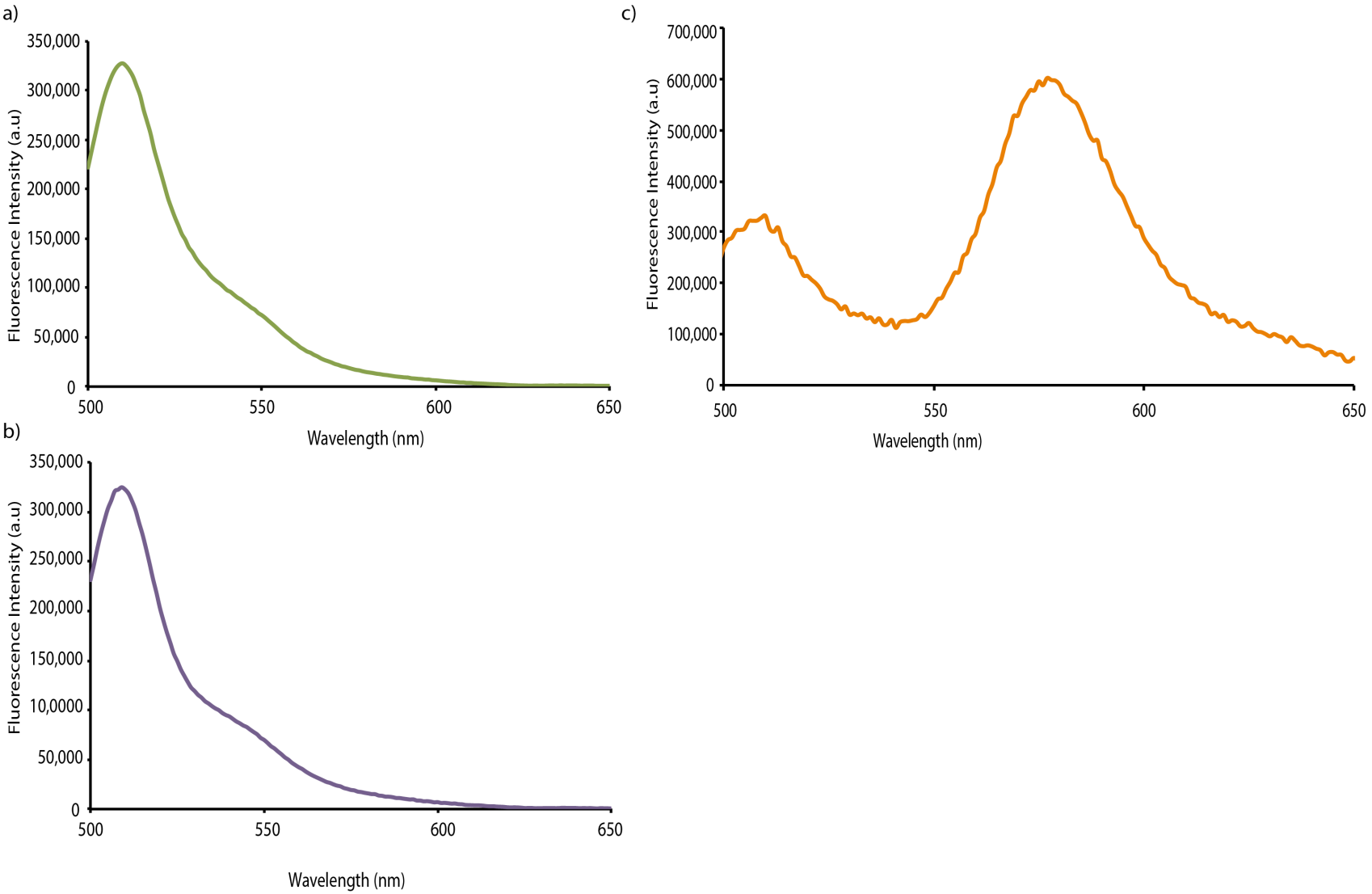

(a) Fluorescence emission spectrum of EGFP (1 μM) (donor FRET pair) (EGFP, Ex/Em 488/508 nm) excited at 488 nm. The spectrum show an intense emission peak at around 510 nm and a small shoulder peak around 548 nm (b) Fluorescence emission spectrum of a solution of EGFP (1 μM) and dfTAT (5 μM) (acceptor FRET pair) (TMR, Ex/Em 556/580 nm) excited at 488 nm. The spectrum shows an intense emission peak at around 510 nm and a small shoulder peak around 548 nm. The contribution of TMR to the EGFP fluorescence spectrum (crossover fluorescence) was determined by measuring the fluorescence emission of a solution of dfTAT (5 μM) excited at 488 nm (not shown). The spectrum of the solution with EGFP and dfTAT is almost identical to the spectrum of EGFP alone (TMR fluorescence crossover signal was subtracted). (c) Fluorescence emission spectrum of ligated EGFP-CK(TMR). Using expressed protein ligation, EGFP was chemically ligated to CK(TMR) as described to produce EGFP-CK(TMR)7. EGFP-CK(TMR) was used a positive control for the FRET signal. Upon excitation at 488 nm, a dramatic increase in fluorescence between 560-630nm is observed (fluorescence max approximately 580 nm), indicative of a FRET signal due the close proximity between fluorophores. This increase in fluorescence intensity was not observed in the spectrum in part b) (indicative of no interactions between EGFP and dfTAT). Emission of all samples was scanned from 500 to 650 nm.

Figure S28. dfTAT does not interact with EGFP.

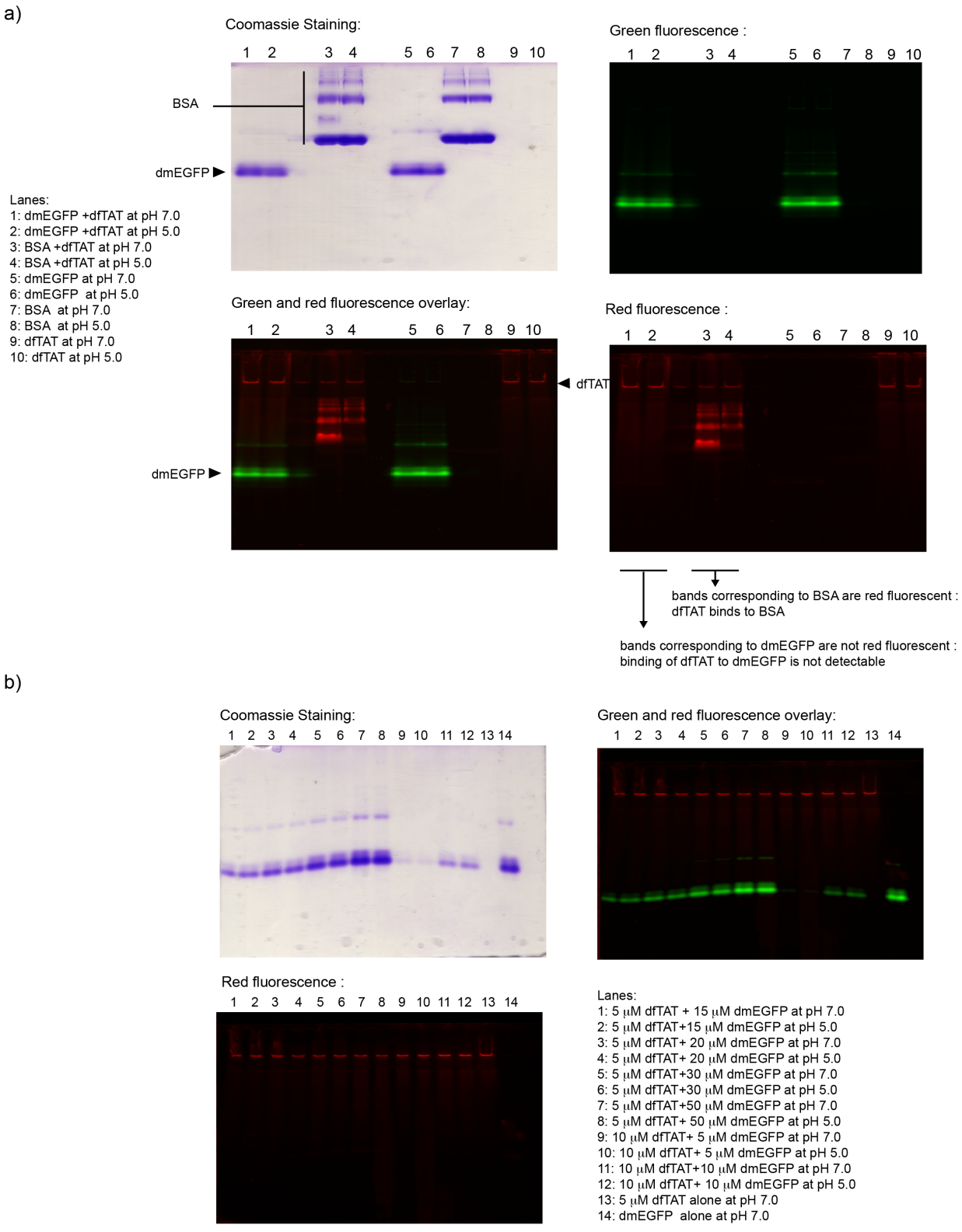

(a) Native gel electrophoresis was used to determine binding interaction between dfTAT and EGFP. Samples were prepared by incubating dfTAT (5 μM) with either EGFP (10 μM) or BSA (10 μM, protein with a pI = 4.7, used as a positive control) in nrL-15 for 30 min at 37 °C (pH 7.0, representing the pH of the extracellular milieu of the cell and pH 5.0 representing the lower pH that exists along the endocytic pathway). dfTAT alone, EGFP alone and BSA alone at the same concentration and pH were loaded on the same gel as controls. Fluorescence Images of the gel were acquire using a Typhoon scanner. Green fluorescent bands correspond to EGFP and red fluorescence band correspond to dfTAT fluorescence. Red fluorescent bands corresponding to both dfTAT and BSA indicate binding between peptide and protein. In contrast, dfTAT fluorescence is not detected in bands corresponding to EGFP, indicating absence of binding. An image of the commassie stained native gel is also shown (top left corner). (b) Coomassie staining, red fluorescence, and green fluorescence images of samples of dfTAT and EGFP at varying concentration and analyzed by native gel electrophoresis. Similar results were obtained with dmEGFP (EGFP not containing cysteine residues, data not shown).

Figure S29. Effect of BSA, heparin and FBS on dfTAT cell penetration

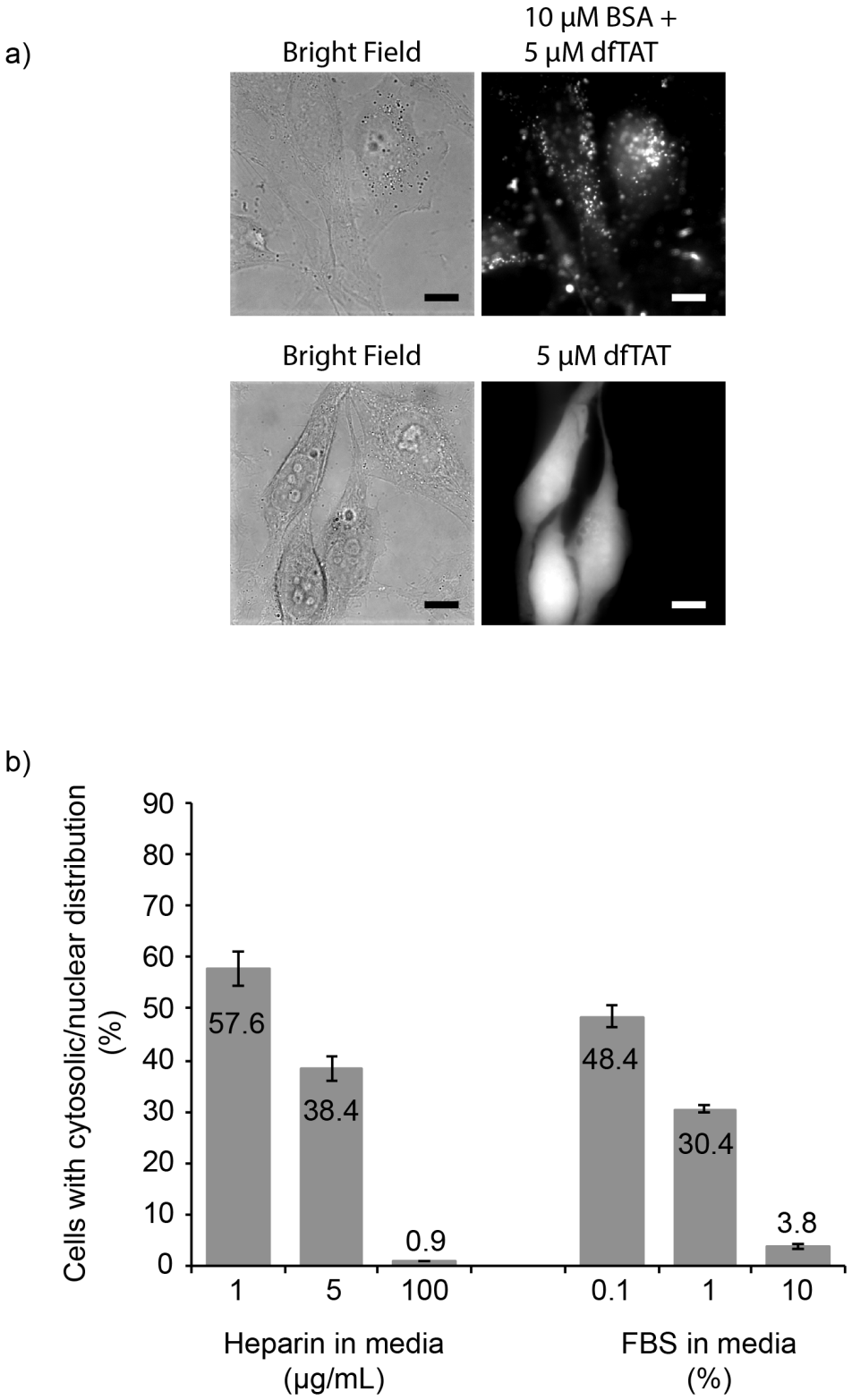

(a) Co-incubation of dfTAT with BSA results in a decrease in the percentage of cells displaying cytosolic release of dfTAT. HeLa cells were co-incubated with 5 μM dfTAT and 10 μM BSA for 1h. Cells show a punctate distribution of the peptide (monochrome 100X image) indicative of peptide being trapped in endocytic vesicles. In comparison, HeLa cells incubated with dfTAT (5 μM) alone show a homogenous cytosolic and nuclear distribution of peptide in a majority of cells. (b) Effect of FBS and heparin on dfTAT mediated cellular. HeLa cells were incubated with 5 μM dfTAT and heparin (1-100 μg/mL) or FBS (0.1-10%) for 1 h. Cells were washed and imaged. The % cells with cytosolic and nuclear distribution was calculated as described in Figure 1(b). Scale bars: 10 μm.

Figure S30. The FITC-anti-ATP5a antibody co-localizes with a fluorescently labeled mitochondrial protein expressed in live cells after dfTAT-mediated delivery.

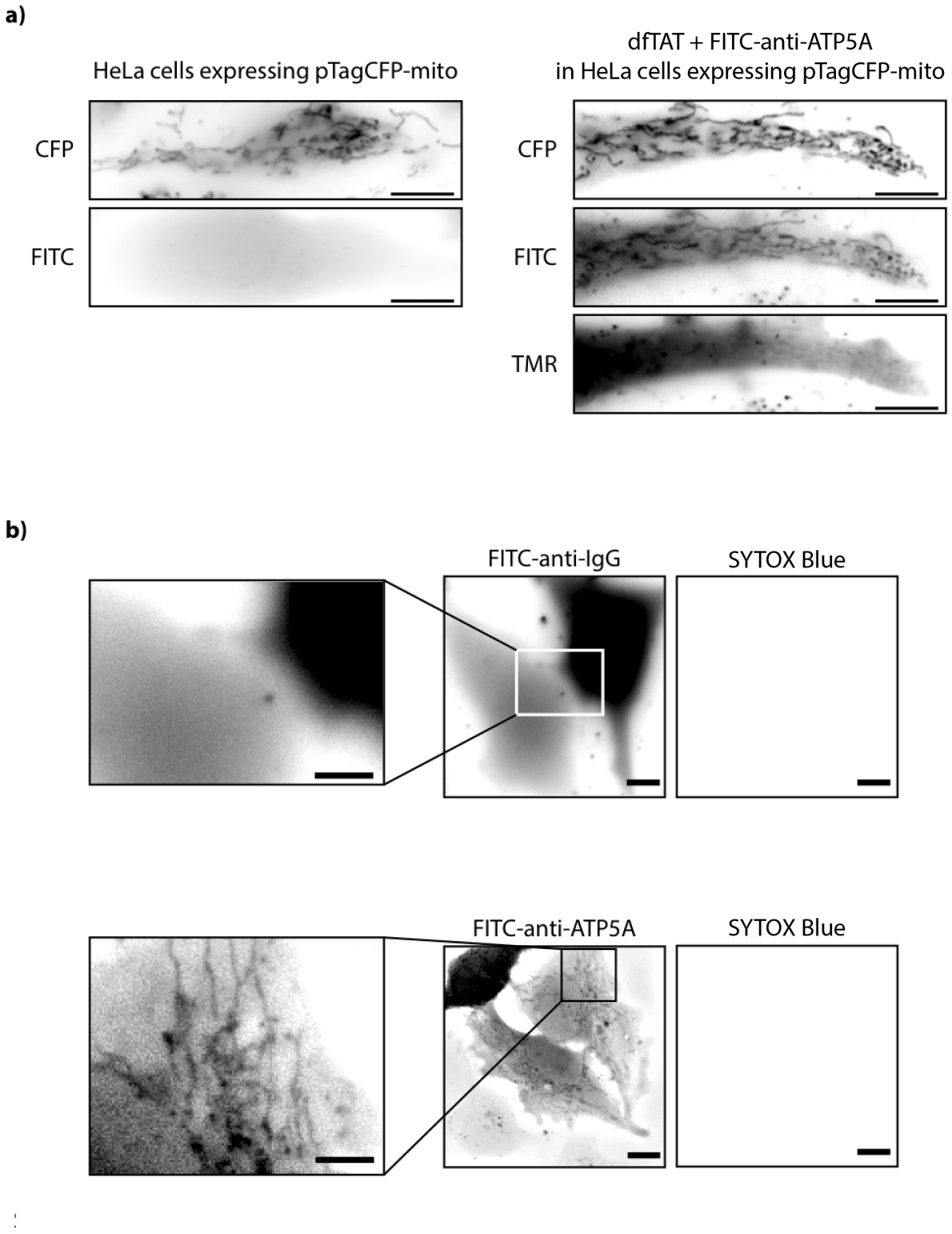

(a) Cells expressing TagCFP-mito (left) were imaged using the FITC and CFP filters. Tubular mitochondria were clearly observed only in the CFP channel. In a separate experiment, dfTAT (5 μM) and FITC-anti-ATP5A (20 μg/mL) were incubated for 1 h with cells expressing TagCFP-mito. The inverted monochrome images show co-localization of FITC-anti-ATP5A (FITC channel) and TagCFP-mito (CFP channel). Scale bars, 2 μm.
(b) To confirm that the mitochondrial staining is specific to FITC-anti-ATP5A, an antibody without an intracellular epitope, FITC-anti-IgG, was delivered with dfTAT. FITC-anti-IgG (20 μg/mL) and dfTAT (5 μM) were incubated with cells for 1 h. Inverted monochrome images show a homogenous cytosolic fluorescence distribution (top). In contrast, cells that were incubated with FITC-anti-ATP5A show fluorescence in tubular structures (bottom). Scale bars, zoom-in image: 2 μm, 100X objective: 10 μm.